universität wien

MASTERARBEIT / MASTER'S THESIS

Titel der Masterarbeit / Title of the Master's Thesis

„The influence of animal age and cutting solutions on the viability of acute spinal cord slices of rats"

verfasst von / submitted by

Alexander Martzok, B.Sc.

angestrebter akademischer Grad / in partial fulfilment of the requirements for the degree of

Master of Science (MSc)

Wien, 2020 / Vienna, 2020

Studienkennzahl lt. Studienblatt / degree programme code as it appears on the student record sheet:	UA 066 878
Studienrichtung lt. Studienblatt / degree programme as it appears on the student record sheet:	Masterstudium Verhaltens-, Neuro-, Kognitionsbiologie
Betreut von / Supervisor:	Mag. Ruth Drdla-Schutting, PhD

Abstract

Acute slices are an important model for research on neuronal circuits. The model is well suited for movement-sensitive electrophysiological recording techniques and pharmacological drug application. However, neuronal tissue can suffer from ischemic injury during slice production. Reports claim that slices from older animals were more prone to ischemic injury resulting in low viability. One of the most effective methods to protect their viability is the modification of the artificial cerebrospinal fluid (aCSF) that is used for cutting and subsequent incubation. A NMDG-HEPES aCSF enriched with antioxidants was proposed to reduce cell swelling, acidification and oxidative stress in the tissue. While already successfully used for preparing healthy brain slices, the beneficial effect of protective cutting protocols for spinal cord slices – if any – is still unclear. In this study, I aimed at testing the effectiveness of a NMDG-HEPES aCSF for preservation of spinal cord slices of adolescent male rats.

Here, a comparison of overall viability of spinal cord slices prepared from young (20–25 days) or adolescent male rats (35–40 days) revealed no differences. Likewise, the electrophysiological properties of neurons in lamina I were similar between the groups. The use of NMDG-HEPES aCSF for slice preparation did not have any beneficial effects on overall health when compared to a modified sucrose aCSF. In contrast, slices showed significantly lower viability, which could be restored by reducing the time of incubation in NMDG-HEPES aCSF. Taken together, NMDG-HEPES aCSF was no more suitable to preserve spinal cord slice viability than traditional sucrose aCSF under our experimental conditions.

1. Table of contents

2. Acknowledgments

First of all, I would like to thank Univ.-Prof. Dr. Jürgen Sandkühler for giving me the opportunity to do my master project at the Department of Neurophysiology.

I am especially grateful for the tireless support by Mira Kronschläger. Her expertise and great advice enabled the success of this project in the first place. She taught me the complex patch-clamp technique and helped me to improve my scientific methods.

Furthermore, I would like to express my gratitude to Ruth Drdla-Schutting for supervising my project and introducing me into the world of patch-clamp.

I would like to thank Bernhard Heinke who improved my project with his valuable input and always helped me with the problems I encountered with the setup and devices.

Of course, special thanks go to the technicians of our department, who supported my experiments by providing materials and advice. I would also express my gratitude to Teresa Haider and Sibel Ada, who had always helpful tips available and time for interesting conversations. I thank Gilbert Janeselli for the IT support of my project.

Finally, I cannot express enough, how thankful I am for the support of my girlfriend Julia Weikel and my parents Manuela and Andreas Martzok. I would not have come this far without them.

3. Introduction

Brain or spinal cord slices are isolated sections of neuronal tissue obtained from an *ex vivo* preparation. Depending on which part of the system is isolated, slices contain different regions of interest. Studies with acute slices of hippocampal (e.g. Knowles and Schwartzkroin, 1981; Konopacki et al., 1987), midbrain (e.g. Cox and Johnson, 1998; Jaffe et al., 1998) or cerebellar (e.g. Egert et al., 2002; Brockhaus et al., 2004) regions as well as spinal cord lumbar segments (e.g. Mitra and Brownstone, 2012; Kronschläger et al., 2016) are only a few examples. Sectioning of neuronal tissue removes most afferent and efferent pathways. Thus, examination of the dynamics of a complete neuronal network is no longer possible. However, cytoarchitectural preserved units and local microcircuits stay mostly intact (Andersen, 1989; Sarvey et al., 1989; Cahalan and Neher, 1992). Acute slices offer two main advantages in contrast to recordings *in vivo*:

1. Slices allow for a high mechanical stability by eliminating the factor of the animal's body movement. This stability enables long recordings with movement-sensitive techniques such as intracellular recordings or patch-clamp recordings (Dingledine et al., 1980).

2. The extracellular environment of an acute slice can be monitored and therefore precisely controlled. Since slices are devoid of the blood-brain barrier, the effect of pharmaceutical drugs or other environmental stimuli can be examined directly (Berger, 1990; Dingledine et al., 1980).

The advantages described above make acute slices a predestined model for electrophysiological studies. Intracellular or patch-clamp recordings offer the possibility to examine the electrophysiological properties of single cells. With microelectrode arrays (Stett et al., 2003; Liu et al., 2012) or calcium imaging (Mainen et al., 1999) it is possible to analyse the activity of small neuronal networks or populations. Furthermore, these methods can be combined with genetic or histological tools. Cells of interest can be identified by fluorescence proteins (Marvizón et al., 1997) or activated via optogenetic manipulation (Ting et al., 2014). Patched cells can be filled with fluorescent dyes applied via the pipette solution and later localised on the slice (Schwartzkroin and Mathers, 1978) and post-hoc characterised by additional stainings. The patch-clamp technique is an ideal method to be applied on acute slices, since cells with an intact cytoarchitecture are easily accessible right below the surface. Patch-clamp recordings allow the measurement of electrophysiological properties of the whole cell membrane or even single ion channels. For electrophysiological measurements, a tight connection with the membrane is established using a glass micropipette. It is filled with a solution mimicking the intracellular solution and coated wire functioning as an electrode. This

recording electrode is connected to a reference electrode that is placed in the outer medium or tissue. The tip of the recording electrode is placed on the membrane surface and a strong suction is applied until the membrane is ruptured. This gives access to the cell interior, establishing an electrical connection between the cytoplasm and the pipette. The potential difference between the recording electrode and the reference electrode is thereby equivalent to the potential between cytosol and the extracellular medium. A current can be injected to hold the potential across the membrane on a desired level (Sakmann and Neher, 1984). The patch-clamp technique thereby allows the precise monitoring of the electrophysiological properties of a cell (Staley et al., 1992). Different stimuli such as drugs can be applied to the external medium to study their effect on cellular membrane properties.

The quality and stability of the patch-clamp recording depends on the overall condition of the cells. Injury or long-lasting energy depletion can impair the cell function. In the worst case, the cell undergoes necrosis leading to degeneration of cell organelles, such as the cell membrane. As a result, the electrophysiological properties are no longer resembling a physiological state. Furthermore, the instability of the cell membrane impedes long lasting and stable recordings. It is therefore important to take steps to preserve slice viability close to physiological level. It is in the nature of things, that tissue slices get injured during the preparation and slicing process. Understanding which types of injuries are inflicted can help to implement protective measurements into the protocol.

To prepare acute slices, the neuronal tissue is removed from its bony cavity. Afterwards, the tissue is fixed on an agar block. From this point in time onwards, the tissue has to be constantly superfused with an artificial cerebrospinal fluid (aCSF). In this way, a stable and physiological environment as well as a sufficient provision in terms of nutrition is ensured (Andersen, 1981). The composition of a typical aCSF proposed in 1989 by Aghajanian and Rasmussen contained (in mM): 126 mM NaCl, 5 mM KCl 1.2 mM $CaCl_2$, 2 mM $MgS0_4$, 26 mM $NaHC0_3$, 1.25 mM NaH_2PO_4 and 10mM D-glucose. The aCSF is additionally oxygenated with 95% O_2/5% CO_2 to ensure supply of oxygen while the CO_2 buffers the medium. Since the supply of the tissue is based on simple diffusion, the thickness of acute slices is limited to ~ 600 µm. The tissue is cut into thin slices using a vibratome. This device drives a thin, sharp blade through the tissue block with minimal vertical vibration. The slices are afterwards incubated in aCSF for a given period of time. This step allows recovery of injured cells and tissue before the actual experiments begin. Nonetheless, without enough precaution the freshly cut tissue is often paved with numerous oedemic cells. These cells are characterised by a round and swollen morphology due to excessive influx of water into the cytosol (Richerson and Messer, 1995).

Slice viability is mainly influenced by three types of injury:

1. Decapitation of the animal and removal of the organ induces an ischemic injury to the neuronal tissue. The time it takes from the anaesthetisation of the animal until the slice is cut and incubated is critical. In this time frame the supply of oxygen and glucose, required for the maintenance of cell function, is gradually impaired. Consequently, internal stocks of ATP will decline due to the limited resources of production. As a result, the failure of the Na^+/K^+-pump will no longer revert influx of Na^+ ions, resulting in a depolarisation of the membrane potential. K^+ efflux can initially compensate for the influx of Na^+, but the concomitant increase in the intracellular Cl^- concentration that is linked to cell swelling establishes an electroneutrality, thus detaining cations in the cell. The resulting hypertonic state leads to influx of water and thereby swelling of the cell. One possible explanation for Cl^- influx is the activation of Cl^- transporters by depolarization. Due to the positive charge of the cytosol, Cl^- follows its electrochemical gradient and flows into the cell (Feig and Lipton, 1990; Siklós et al., 1997; Rungta et al., 2015; Liang et al., 2007).

Depolarisation increases firing rate, activating voltage-dependent calcium channels. The influx of calcium can trigger vesicle fusion and release of glutamate, as long as ATP supplies are not depleted. The re-uptake of extracellular glutamate by neurons and astrocytes is based on the exchange of K^+. Elevated K^+ concentration reverses the re-uptake and glutamate accumulates outside of the cell. The result is a continuous activation of NMDA receptors, thereby initiating further and additional calcium influx into the cells. This might trigger enzymatic activity far above physiological levels resulting in protein breakdown, free radical formation and lipid peroxidation. This process is commonly referred to as glutamate-induced excitotoxicity (Nicholls and Attwell, 1990; Lipton and Rosenberg, 1994; Brahma et al., 2000).

2. Besides the mechanical injury caused by the cutting blade, the movement itself can also induce damage by compressing the already stressed neuronal tissue (Kaneda et al., 1988). This may be caused by the vertical oscillation of the blade resulting in a compression of the tissue below and above. The cutting speed is also important for slice viability. Moving the blade too fast might apply shear forces damaging the neuronal tissue. Liu et al. (1991, 1999) showed that injuries inflicted to the spinal cord can result in accumulation of glutamate and other excitatory amino acids, leading to neuronal cell death due to excitotoxicity.

3. The re-oxygenation of acute slices is achieved by a 95% O_2/5% CO_2 mix supplied to the extracellular medium. Although the reintroduction of oxygen to the slice is necessary to restore cell function, this hyper-oxide environment may induce a so-called reperfusion injury due to

oxidative stress via reactive oxygen species (ROS). An early marker for reperfusion injury is cell swelling. ROS take up electrons from otherwise stable molecules and in this way damage DNA, proteins and the cell membrane. Ischemic tissue has an increased demand for oxygen to restore cell function and energy supply. Beside the reperfusion injury caused by the hyperoxide environment, ROS are a byproduct of ATP-production by oxidative phosphorylation in the mitochondria. The effects of reperfusion injury and increased ROS production cannot be compensated by endogenous antioxidants such as ascorbate or glutathione, which act as reducing agents under physiological conditions. While ascorbate as a vitamin is taken up from the blood plasma, glutathione is directly produced in cells under physiological conditions. However, both supplies are diminished during acute slice preparations due to the ischemic injury and are also washed out during the incubation of the slices (Sasaki et al., 2018; Rice, 1999; Brahma et al., 2000).

Each of these pathways described above can influence the overall slice condition. In addition, they are interdependent and can reinforce each other. Excessive activation of glutamate receptors and consequent calcium influx has been shown to depolarize mitochondria and increase calcium-dependent ROS production (Dykens et al., 1987; Prehn, 1998; Trotti et al., 1998). Vice versa, ROS can impair the reuptake of glutamate via glutamate transporters in neurons and astrocytes, thereby supporting excitotoxicity (Volterra et al., 1994; Trotti et al., 1998; Rao et al., 2003). Furthermore, glutamate receptor activation (Hartley and Dubinsky, 1993; Brune and Deitmer, 1995) as well as ROS activity (Tsai et al., 1997) can induce an acidification of the cell, which seems to enhance the oedemic reaction (MacGregor et al., 2001). Acidification of the tissue in turn can reduce the reuptake of glutamate (Swanson et al., 1995).

Thus, slice viability can be greatly improved by preventing 1. the formation of Na^+- and Cl^--induced oedema, 2. the protein breakdown by ROS activity and 3. the acidification of the extra- and intracellular medium.

It seems that acute tissue slices from older rodents are especially vulnerable to the described injuries inflicted by the preparation. This has been attributed to a higher vulnerability to injury and stress in older compared to younger animals (Tanaka et al., 2008; Huang and Uusisaari, 2013; Ting et al., 2014, 2018).

The lower resistance to ischemic injury of older brains has been attributed to a decline in the antioxidant defence system. More markers of oxidative stress, such as protein carbonyl content, were found in brain tissue of aged in comparison to younger animals. Furthermore,

activity of antioxidants and protective enzymes decreased in the later adult stages. Occurrence of oxidative stress markers and a drop of cognitive performance after a traumatic brain injury were more severe in aged than in young adults (Tian et al., 1998; Navarro et al., 2002; Itoh et al., 2013).

Hippocampal mitochondria of neonatal rats (P 3–6 days) are more resistant to hypoxia-induced depolarisation than mitochondria of adolescent rats (P 35–42 days) (Larsen et al., 2008). Isolated mitochondria from the cortex of intermediate (12–14 months) and aged (22–24 months) adult rats show more signs of damage from ROS than the young adult group (3–5 months) (Gilmer et al., 2010). Roberts, Jr. and Chih showed (1997) showed that pH-regulation is impaired in aged adult rats (24–27 months) in comparison to young adults (6–8 months).

In experiments with mice, a hypoxic-ischemic injury was induced in animals on P 5, 9, 21, 60. Injury duration was shortened with increasing age, to achieve a similar degree of injury in form of tissue hypertrophy and cell infraction in all age groups. This indicates a higher resistance of younger animals against pure hypoxic damage in comparison to young adults (Zhu et al., 2005). In other studies, a high resistance to ischemic injury induced by carotid ligation or glutamate injection was, in contrast, only observed in neonatal rats up to P 2–5. The occurrence of lesions, strokes and other markers of ischemic injury drastically increased at P 6–7 and this vulnerability was shown to extend until P 30. Brains of neonatal rats around P 6–7 seem to suffer more from glutamate-related excitotoxic pathways, compared to those from older age groups (Ikonomidou et al., 1989; Blumenfeld et al., 1992; Grafe, 1994; Yager et al., 1996; Towfighi et al., 1997; McDonald et al., 1988). These findings contradict other studies, reporting higher resilience to hypoxic damage in acute slices obtained from young compared to older animals (Tanaka et al., 2008; Mitra and Brownstone, 2011; Ting et al., 2018).

A number of recent studies have validated different methods for enhancing neuronal preservation and overall viability in acute brain slices from adult rodents. The most common strategy is the modification of the aCSF to intercept injury pathways. One of the first changes applied to the original solution was the substitution of NaCl with sucrose (in mM): 252 mM Sucrose, 5 mM KCl 1.2 mM $CaCl_2$, 2 mM $MgSO_4$, 26 mM $NaHCO_3$, 1.25 mM $NaHOPO_4$ and 10mM D-glucose. Its purpose was to prevent cell swelling caused by influx of Na^+ and Cl^- ions while maintaining the osmolarity of the extracellular solution (Aghajanian and Rasmussen, 1989). Since then, numerous other substitutes for NaCl, such as choline, glycerol or N-methyl-D-glucamine (NMDG) were empirically tested and their preservative effectiveness compared to each other (Richerson and Messer, 1995; Tanaka et al., 2008; Ye et al., 2006; Ting et al., 2014). Although an early study did not show any advantage of NMDG over sucrose aCSF

(Richeron and Messer, 1995), recent comparisons suggest a better ability to preserve cell morphology (Ting et al., 2014; Pan et al., 2015; Avegno et al., 2019) and neuronal survival (Tanaka et al., 2008). Furthermore, to reduce the excitotoxic effects of glutamate receptor activity and the subsequent calcium influx, a low-calcium aCSF combined with kynurenic acid to antagonise NMDA receptor activation is frequently used. This increases the survival time and rate of neurons in comparison to aCSF or sucrose aCSF (Richerson and Messer, 1995). Supplementation of endogenous antioxidants such as ascorbate and glutathione to the aCSF causes effects comparable to those of NMDA receptor antagonists. Thiourea is an exogenous reductive agent, which seems to further improve protective effects of ascorbate (Brahma et al., 2000; Ting et al., 2014; Anzini et al., 2010). Slice condition might also be improved by adding 4-(2-hydroxyethyl)-1-piperazineethanesulfonic acid (HEPES) to the extracellular medium to buffer the acidification of cells caused by calcium influx (MacGregor et al., 2001; Ting et al., 2014). A NMDG-HEPES aCSF enriched with antioxidants, combining the protective measurements described above, was proposed by Ting et al. in 2014. To date, this solution is used in several research groups working with acute brain slices of adult animals (Ting et al., 2018).

In our research group, we are studying central nervous system mechanisms of pain, i.e. at the spinal cord level. The spinal cord functions as a relay station between the peripheral and central nervous system. It has two functionally distinct areas: 1. The grey matter consisting of neuroglia cells and neuronal cell bodies with dendrites and mostly unmyelinated axons. 2. The white matter consisting of both myelinated and unmyelinated axons and neuroglia cells. Axonal tracts from spinal cord grey matter neurons and the brain act as an information highway between each other. The grey matter can be separated into a ventral and dorsal horn (Bican et al., 2013). The dorsal horn is divided into six laminae, based on their cellular structure and the termination pattern of afferent fibres (Rexed, 1954). Peripheral, primary afferents with innervations from the skin or deeper tissue transmit information via the dorsal root ganglions to the different layers of the dorsal horn. Lamina I and II are involved in nociceptive information processing. The nociceptive signals are primarily conducted by unmyelinated C-fibres and thinly myelinated Aδ-fibres (Todd, 2010). Aβ-fibres innervating lamina 3 to 6 carry information from mechanoreceptors in the skin and joints. Aα-fibres originate from muscles spindles and golgi tendons and innervate the lamina 6 as well as the ventral horn. Projection neurons from the dorsal horn form ascending tracts to the white matter, transmitting processed information of peripheral sensation to the brain (Bican et al., 2013). In our studies, we routinely use transversal spinal cord slices with dorsal roots attached. We investigate modulations of nociceptive transmission between C- and Aδ-fibres and dorsal horn neurons using an

electrophysiological approach. We are especially interested in deciphering the detailed mechanisms of activity-dependent and -independent forms of synaptic plasticity in nociceptive pathways (Drdla et al., 2009; Gruber-Schoffnegger et al., 2013; Kronschläger et al., 2016; Reischer et al., 2020). Such sophisticated neuronal recordings require optimal slice conditions and therefore protective measurements should be implemented wherever necessary.

In our own experience, acute spinal cord slices obtained from adolescent rats or mice seem to be more vulnerable to the cutting procedure. These slices often seem to contain a lower number of healthy cells suitable for electrophysiological recordings compared to slices from younger animals. Furthermore, depolarised membrane potentials of neurons have been frequently observed in these slices, which is an indicator of impaired cell function. Most of the viability-preserving methods were so far mainly established for brain slices. It is currently unknown whether the use of protective cutting solutions such as NMDG-HEPES aCSF has a beneficial effect on the viability of acute spinal cord slices from older animals.

3.1. Aim of the study

Since an objective comparison of viability in spinal cord slices from different age stages is missing to date, the first aim of the study was to investigate whether slice tissue from young animals (P 20–25) were more vulnerable to injuries than slices from adolescent animals (P 35–40). To assess overall slice viability, I first determined the morphology of neurons residing in lamina I of the dorsal horn. To assess overall slice condition and recording stability, I measured electrophysiological properties of the neurons in lamina I using the whole-cell patch-clamp technique.

The second aim of this study was to test if a NMDG-HEPES aCSF was in general superior in preserving the overall slice viability compared to an established sucrose aCSF. A good slice condition ensures a high number of cells available for electrophysiological recordings, reducing the number of animals necessary for an adequate sample size. The choice of preparation methods and techniques is thereby highly relevant for animal welfare and project management. Slice viability and neuronal electrophysiological properties were assessed in the same way as in the age stage comparison.

In summary, in this study I aim to answer the following questions:

1) Is there a quantitative difference between the viability of spinal cord slices from young and adolescent animals?

2) Can the use of NMDG-HEPES aCSF preserve spinal cord slice viability better than sucrose aCSF?

4. Methods

4.1. Animals

Experiments were performed on male Sprague Dawley rats from the in-house animal husbandry of the Center for Brain Research of the Medical University of Vienna (Vienna, Austria) or from the Institute for Experimental Animal Breeding of the Medical University of Vienna (Himberg, Austria). Rats were group-housed under a 12-hour light/dark cycle. The temperature and relative humidity were kept at 22 ± 2 °C and 55 ± 10% respectively.

In general, rodents are roughly categorised in the following age groups (postnatal days P): neonatal P 0–7, young P 8–34, adolescent P 35–62, young adult 2–6 months, intermediate adult 6–18 months and aged adult >18 months. In the present study, we used animals from two different age groups: animals aged 20-25 days were considered young, whereas animals aged 35-40 days were considered adolescent. The age of the animals used is stated clearly in the results and in the figure legends. All experimental groups were intermingled. Thus, potential confounding factors should have influenced all groups equally.

4.2. Preparation of acute spinal cord slices

4.2.1. Standard group

All rats were deeply anesthetised with isoflurane, weighed and securely fixed on a preparation plate. A paw pinch reflex test was applied to determine sufficient depth of anaesthesia. The animals were sacrificed by decapitation and a laminectomy was performed under a binocular. The exposed spinal cord was cut, removed and pinned on a silicone plate filled with crushed-ice standard aCSF which was previously oxygenated with a carbogen mixture of 95% O_2/5% CO_2. As a next step, the dura and the ventral roots were removed using microsurgical scissors and forceps. The segments from L1–L5 were cut and glued ventrally onto an agar block fixed perpendicular in the slicing platform of a DTK-1000 Zero 1 vibratome (Dosaka EM CO., LTD). The platform was filled with the ice-cold standard aCSF oxygenated with a carbogen mixture of 95% O_2/5% CO_2. The spinal cord was cut into transversal slices of approximately 400 µm

thickness. Six to eight slices with the dorsal root attached were obtained. Finally, the slices were incubated for 30 min in standard aCSF oxygenated with a carbogen mixture of 95% O_2/5% CO_2 at 34°C followed by 30 min incubation at room temperature.

Different solutions for different steps of the preparation process were tested in this study and compared to the standard group. A graphical depiction of the preparation steps and solutions used in the different groups is shown in **Fig. 1** and described below.

4.2.2. NMDG group

Here, crushed-ice NMDG-HEPES aCSF was applied during the laminectomy and during the slicing of the spinal cords. Additionally, the slices were allowed to recover for 15 min in NMDG-HEPES aCSF at 34° C (= recovery period). Slices were then transferred into standard aCSF for 15 min at 34°C (**Fig. 1** NMDG). Afterwards, the slices were incubated for at least 30 min in standard aCSF at room temperature until further use. The experimenter was blinded for the solution used for each animal until the data was analysed.

4.2.3. NMDG-recovery only group (NMDG-r)

To evaluate how short exposure of the spinal cord slices to NMDG affects their viability, the preparation was further modified. Here, all steps up to slicing of the spinal cord were performed in standard aCSF. The slices were then transferred into NMDG-HEPES aCSF for a 15 min recovery period at 34° C and subsequently incubated for 15 min in standard aCSF at 34° C. This was followed by a 30 min incubation at room temperature (**Fig. 1** NMDG-r). The experimenter was blinded for the solution used for each animal until the data was analysed.

	Preparation step					aCSF
Group	~ 8 min	~ 35 min	~ 30 min	30 min at 34° C		
Standard	Laminectomy	Spinal Cord Preparation	Slicing	Incubation		Standard aCSF
NMDG	Laminectomy	Spinal Cord Preparation	Slicing	Recovery	Incubation	NMDG - HEPES aCSF
NMDG - r	Laminectomy	Spinal Cord Preparation	Slicing	Recovery	Incubation	

Fig. 1 Overview of the preparation steps and solutions used for every group tested. For spinal cord slices in the standard group laminectomy, preparation of the spinal cord, slicing and the incubation period were performed with standard aCSF. For the NMDG group, laminectomy, spinal cord preparation and slicing was performed with NMDG-HEPES aCSF. The incubation period was divided in 15 min recovery in NMDG-HEPES aCSF and 15 min incubation in standard aCSF. For the NMDG-r group the laminectomy, spinal cord preparation and slicing was performed with standard aCSF. The slices were afterwards recovered for 15 min in NMDG-HEPES aCSF and then incubated for another 15 min in standard aCSF. The last preparation step (30 min incubation in standard aCSF at room temperature) is not displayed here, since it was the same for every group.

4.3. Viability assay

To visualise slice viability and measure electrophysiological properties, a slice was placed into the bath chamber of the patch-clamp setup and permanently super-fused with recording aCSF oxygenated with a carbogen mixture of 95% O_2/5% CO_2. To prevent movement of the slice, it was weighted with a nylon mesh fixed to a silver frame. The root was placed in a suction electrode connected to an isolated current stimulator (A 365, World Precision Instruments). The dorsal horn was visualised with Dodt infrared optics using a 40x 0.8 NA water immersion objective on an Olympus BX50WI upright microscope (Olympus, Japan) connected to a TILL camera system. Cells of interests were neurons in lamina I of the grey matter. The slice was exposed to recording aCSF for at least ten minutes before the start of the assay. Healthy cells showed a barely visible soma with an inconspicuous, asymmetrical shape (**Fig. *2*** A). In contrast, cells damaged by the slicing process and/or due to ischemic injury were oedematous and showed a round, swollen and plastic soma (**Fig. *2*** B). Cells which fulfilled the criteria for a healthy morphology were counted and categorised as patchable. Slice viability was quantified by the sum of patchable cells in lamina I.

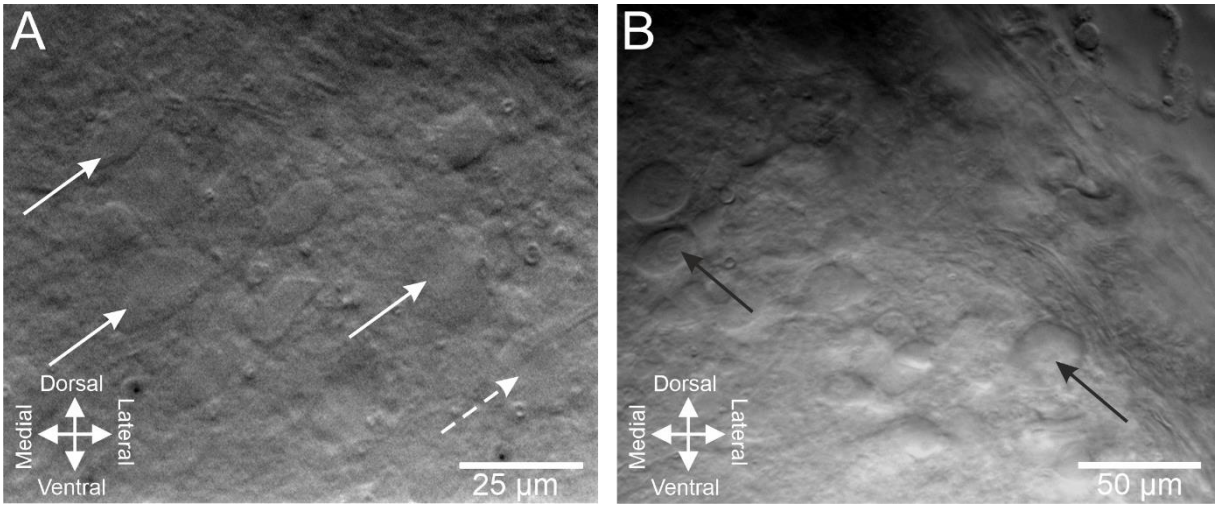

Fig. 2 IR-DIC images of spinal cord slice surfaces obtained from adolescent rats to illustrate two different states of viability in the dorsal horn. A healthy slice is shown in (**A**). Neurons show an inconspicuous, asymmetrical morphology with barely visible nuclei (white arrow). Ideally, the cell is integrated into the surrounding tissue and difficult to detect from the background (white dashed arrow). In **B**, a slice in bad condition is shown. Many cells are oedematous with a clearly delineated plastic edge and visible nuclei (black arrows).

4.4. Electrophysiological recordings of neurons

Recording of basic electrophysiological properties

A randomizer web app (Random Numbers from numbergenerator.org) determined a selection of five candidates from the healthy cells of lamina I (categorised in the viability assay). This measurement was taken to prevent any bias. However, if the number of counted cells did not exceed seven, five of them were patched at will from medial to lateral. If a patch failed, the next cell in line was recorded. The basic electrophysiological properties (i.e. RMP, AP amplitude, dorsal root input) of each cell were recorded.

Recording of synaptic transmission

sEPSC were recorded for 15 min to evaluate the stability of synaptic transmission under different experimental set-ups (i.e. different age groups or different solutions). A maximum of two cells per slice was recorded. Only cells with a RMP more negative than -50 mV were included.

All recordings were performed at room temperature. Whole-cell patch-clamp recordings were performed with a glass pipette filled with a potassium gluconate solution (in mM: potassium gluconate, 120; KCl, 20; $MgCl_2$, 2; HEPES, 20; Na_4-EGTA, 0.5; Na_2-ATP, 2; Na-GTP, 0.5; pH 7.4, osmolarity 280–300 mOsmol/l). Micropipettes were pulled with the horizontal type Flaming/Brown Micropipette Puller Model P-97 (Sutter Instrument CO.) and tip resistance ranged from 2.5–4.5 MΩ. The pipette tip was gently placed on top of the cell of interest. A gentle and continuous suction pressure was applied to establish a giga-ohm seal. With a short but intense suction pressure, the cell membrane was ruptured to gain access to the cell in a whole-cell configuration. Data was sampled at 20 kHz with a low-pass Bessel filter between 2–10 kHz and analysed offline using the pClamp 10.6 software (Molecular Devices). Command potential and currents were achieved using a MultiClamp 700B amplifier (Axon instruments) connected to a Digidata 1440A digitizer (Molecular Devices).

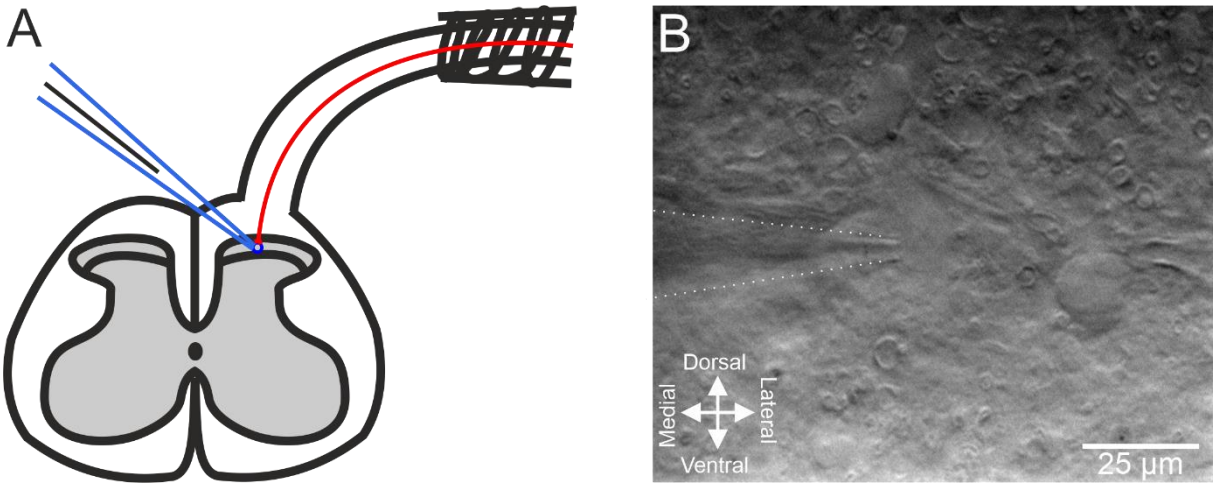

Fig. 3 Spinal cord slice in a patch-clamp configuration. A The dorsal root is placed in a suction electrode. When electrical current is flowing between the electrodes at the root, the change of the electrical field elicits action potentials in the central axons of peripheral neurons (red). The APs are conducted along the nerve fibre, eventually evoking a postsynaptic current in neurons in lamina I. Their electrophysiological activity and properties can be measured via a patch-clamp recording (blue). **B** The surface of the spinal cord slice close to the dorsal transition from grey to white matter. The pipette tip (white dashed line) was placed gently on top of a cell in lamina I to establish a whole-cell patch configuration.

4.4.1. Basic membrane properties

The RMP was measured in current clamp mode. To determine the quality of a patch, a membrane test was conducted. Therefore, in voltage-clamp mode 20 consecutive hyperpolarizing voltage steps from -70 to -80 mV were applied. The voltage change induced a transient current peak which decreased exponentially due to the capacitive nature of the membrane. The initial transient current (I_{Peak}) was used to calculate the serial resistance (R_S) (***Box 1*** B). Since R_S will reduce the effective potential applied at the membrane and can introduce a millisecond time delay for voltage changes at its capacitive element, a low R_S is highly recommended (Molleman, 2003). Only recordings with an initial R_S lower than 30 MΩ were analysed.

Box 1 The structure and behaviour of the cell membrane in a resistor-capacitor element (RC) in a whole-cell patch-clamp circuit.

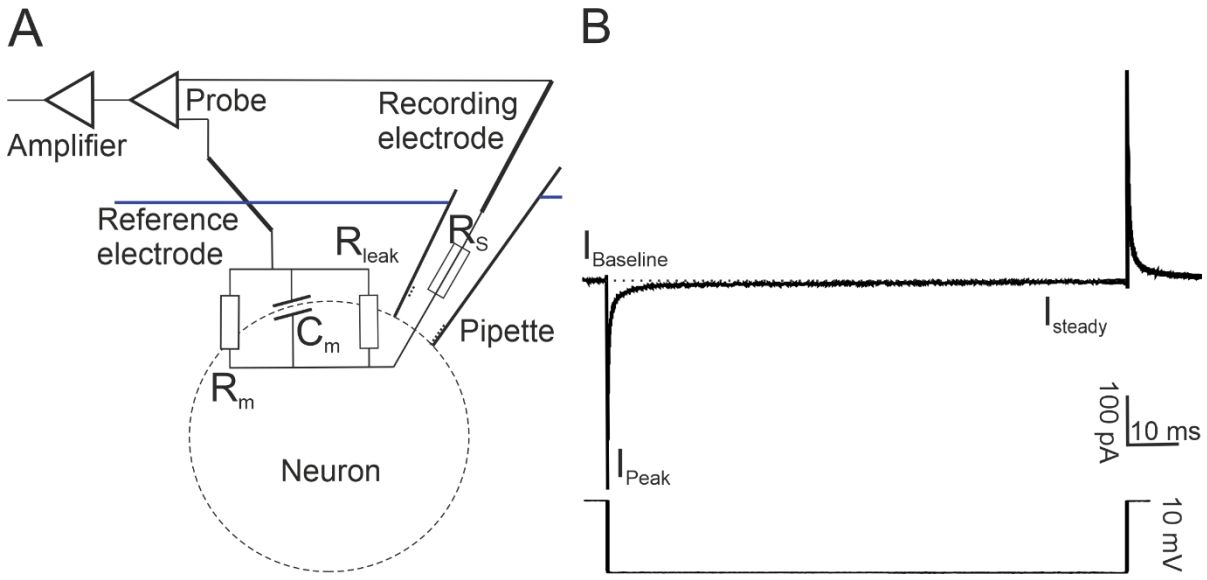

A Since ions cannot freely cross it, the phospholipid bilayer of the cell membrane acts as an insulator between the cytosol and the extracellular medium. It thereby acts as a capacitor (C_m), on which ions accumulate due to the electrochemical gradient of the cell. The resulting charge, which cannot flow across the insulator results into a potential across the capacitor. The only ways to pass the bilayer are the ion channels and pumps. They are acting as resistor elements (R_m). If a whole-cell patch-clamp is established at the membrane, the cell forms a circuit with the reference and recording electrode, each connected to the probe. The probe is the element in which the potential difference between both electrodes can be measured. In an ideal scenario, this potential would resemble the RMP across the membrane. The experimenter can set a command potential to artificially set the RMP at a desired value. To achieve that, the amplifier, which is connected to the probe, compares the measured potential to a command potential. If there is a difference, the amplifier clamps the desired command potential between the electrodes. This results into a current injection into the cell and charges the capacitor element C_m of the membrane. Every current injection necessary to keep the potential at the desired level equals the currents which flow across the membrane. The patch-clamp recording enables to measure membrane potential when no current is injected, or otherwise measure current events across the membrane. The resistance at the pipette tip influences the effectiveness of this feedback system. The magnitude of R_S is mostly determined by the diameter of the tip and also depends on how clogged the tip is by organic tissue remaining from the patch process. It should be kept as low as possible.

Any voltage step applied by the command potential to the circuit will drop at any serial element across the circuit. The voltage drop at R_S will be lost for the potential across the capacitor element of the membrane. Additionally, the time it takes to load the capacitor C_m to its full potential depends on its capacitance and the magnitude of R_S. This RC time constant (called tau) indicates how much time is needed to load charge on the capacitor from 0 to 63.2% of its maximum potential ($\tau = RC$). A high R_S will introduce time delays for the current injection and thus will render the feedback system between membrane potential and command potential less precise. Another factor to consider is the stability of the membrane. Leakage of ions across the membrane (a low R_{Leak}), especially along the rim of the tip where damages may have occurred, would result into a loss of current injection flowing into C_m and thus in another charging delay (Molleman, 2003). **B** A hyperpolarizing voltage step can be used to probe the properties of the individual electrical elements of the patched circuit. As a result of the zero resistance of the capacitor element at the beginning of the step, all current will flow over R_S on the capacitor. Thereby the amplitude of I_{Peak} is only determined by the size of R_S, which is calculated by $R_S = \Delta U/I_{Peak}$. The lower R_S the higher the initial transient current. Since the capacitor's resistance gets close to infinity when fully charged, all remaining current flows over R_S and R_m, the latter being determined by ion channels and transporters of the membrane. It therefore follows that $R_m = \Delta U/I_{steady}-R_S$. The area under the curve of the current can be used to calculate the capacitance C_m. After the voltage step ends, the capacitive element of the membrane will discharge again, resulting into a transient current into the other direction until only the baseline current is restored.

4.4.2. Action potential amplitude

Action potential (AP) amplitude was recorded in current-clamp mode with the membrane potential set to above -80 mV by an appropriate current injection. Stepwise cumulating 20 pA currents were injected into the neuron to elicit action potentials. The amplitude was measured at the first detected action potential. The base was set at the point, where the depolarization triggered a fast ascending action potential. The amplitude was measured from the base point to the highest value of the peak (Figure **Fig. *4*** B).

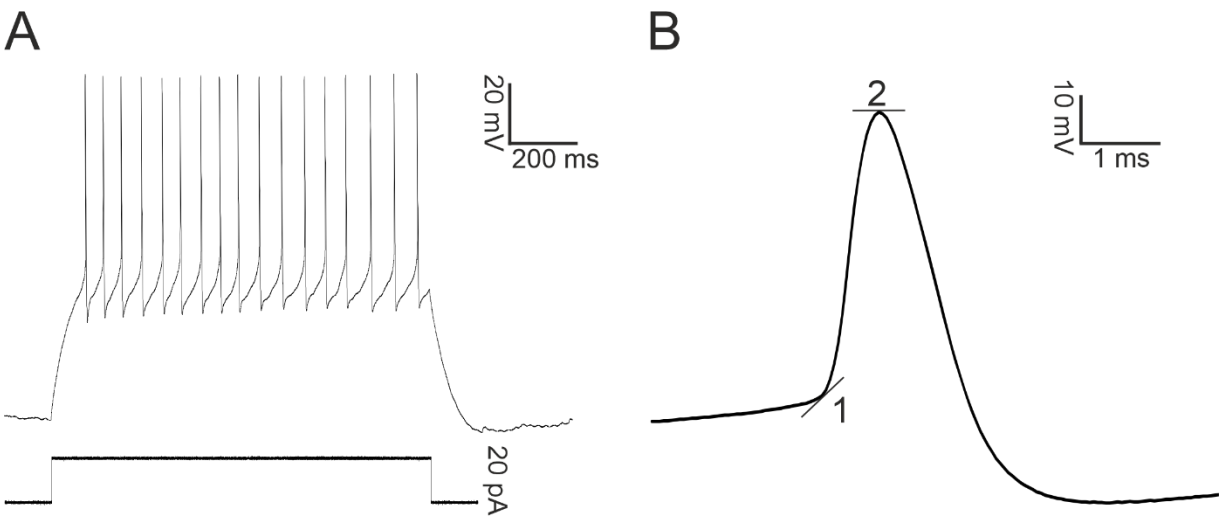

Fig. 4 Morphology and measurement of action potentials elicited in current-clamp mode. **A** The cell was depolarized via current injections with increasing strength until the depolarization surpassed the threshold and action potentials were elicited. The firing pattern varied between single action potentials and bursts of spikes. **B** The first occurring spike was measured to determine its amplitude. The basepoint (1) was set at the point where the slower increasing depolarization changes into the fast rising slope of the triggered action potential. The amplitude was measured from the basepoint to the top of the peak (2).

4.4.3. Evoked excitatory postsynaptic currents

Every recorded cell was tested for synaptic input induced by stimulation of peripheral Aδ- and C-fibre afferents in form of evoked EPSCs (eEPSC). Ten consecutive stimulations of the attached dorsal root via the suction electrode at 10 Hz (Aδ-fibre) and 2 Hz (C-fibre) were applied. The resulting currents were recorded in voltage-clamp mode. Recorded cells were divided into two categories: Cells which received input of any type and cells without any input. The number of cells with input in proportion to the overall number of recorded cells were compared between different groups.

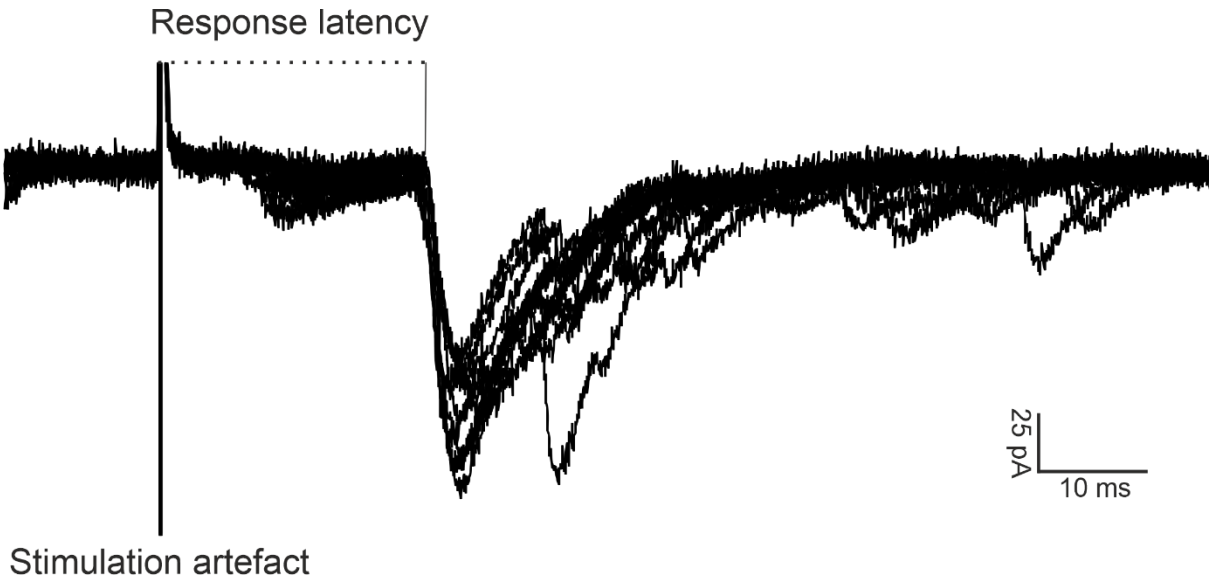

Fig. 5 Overlay of ten consecutive eEPSC recordings. The response latency is measured from the point in time when the stimulation artefact occurs until the beginning of the eEPSC. In this example a C-fibre input is shown.

4.4.4. Spontaneous excitatory postsynaptic currents

To analyse sEPSC, currents were recorded for 15.5 min in voltage-clamp mode at a command potential of -70 mV. In 30 s intervals, a membrane test was applied to control serial resistance over time. The holding current was used as a baseline and determined by the height of the current at the beginning of each membrane test. Only recordings in which the serial resistance did not deviate more than +/- 20% from the initial value were used for further analysis. Amplitude and the number of spontaneous currents were measured for three time intervals: 0–3 min, 6–9 min and 12.5–15.5 min. Only the last 20 s of each 30 s interval were taken into account as the membrane test was cut from each sweep, resulting into a trace length of 120 s per interval. A template to detect sEPSC events was created in Clampfit by merging the curve shape of 20 sEPSC manually (**Fig. *6*** B). A template was created for each time interval separately. The amplitude for each event was determined by the difference from the baseline to the peak of each current. The overall number of events was counted and divided by the recording time in seconds to get the average rate of events per second for each time interval per cell.

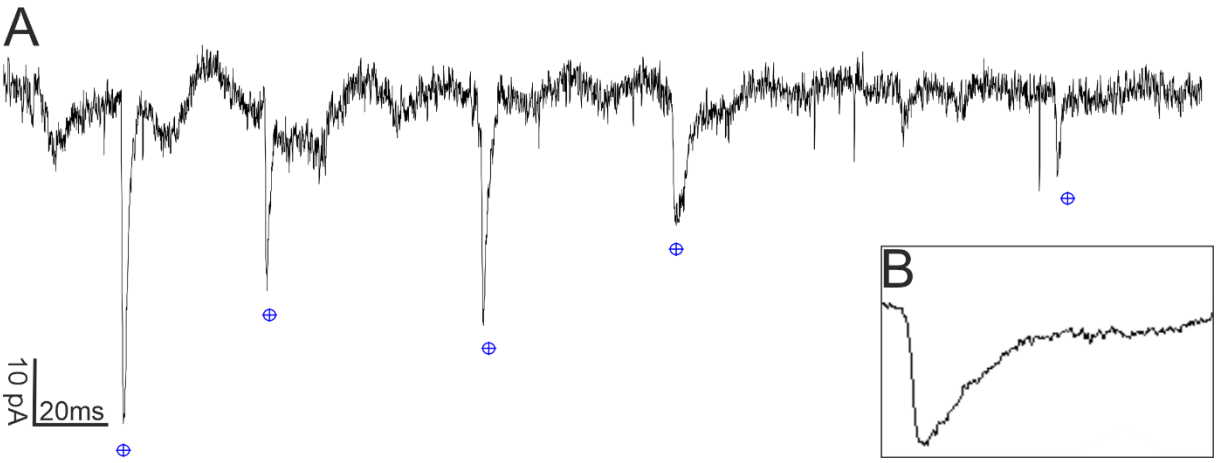

Fig. 6 Detection and measurement of sEPSC recorded in voltage-clamp mode. A Every inward current fitting to the template (**B**) was detected as an event and its amplitude was determined. **B** The corresponding template, which was merged out of 20 manually selected sEPSCs from the original trace.

4.5. Preparation of artificial cerebrospinal fluid (aCSF)

Three different aCSFs were used in this study: a standard preparation aCSF (**Table 1**), a NMDG-HEPES aCSF (**Table 2**) and a recording aCSF (**Table 3**). The lab's standard aCSF is a modified version of the sucrose aCSF first proposed by Aghajanian and Rasmussen (1989). The standard aCSF solution has only a partially substitution of NaCl with sucrose. The purpose of this solution was to protect the slice tissue during the preparation against Na^+-induced oedema formation. For electrophysiological recordings, acute slices were transferred into the recording aCSF. Since neuronal activity highly depends on a certain ion homeostasis, the recording aCSF contained ions in a concentration similar to the physiological extracellular environment. The purpose of this solution was to uphold physiological cell functions during the electrophysiological recordings.

To make the standard preparation and recording aCSF, substances were weighed and dissolved in purified, double-distilled water. Afterwards, stock solutions were added at a calculated volume. The solution was stirred with a magnetic stirrer until all substances were dissolved. After adjusting the finale volume, the osmolarity of the solution was controlled with an osmomat (030 Gonotec GmbH). The acceptable range was set to 305–320 mOsmol/l.

NMDG-HEPES aCSF was made according to the protocol of Ting et al. (2018). Substances were weighed and dissolved in purified, double-distilled water. After all substances were in solution, the pH-value was monitored with a pH-meter (766 from Knick Elektronische Messgeräte GmbH & Co. KG). Approximately 8 ml 10 M HCl were slowly added until the pH

was in a range of 7.3–7.4. Next, the stock solutions were added. Purified, double-distilled water was used to fill it up until the finale volume was reached. The solution was stirred until all streaks disappeared. Only then, the osmolarity was measured with an osmomat. The acceptable range was 308–312 mOsmol/l. Since the osmolarity often ranged at 300 mOsmol/l, sucrose was added until the osmolarity ranged between 308–312 mOsmol/l. All solutions were stored at a temperature of +4° C until further use. Solutions were discarded after max. 3 days. The colour of the NMDG-HEPES aCSF changed to yellow after several days. This seems to be caused by Na-ascorbate (Ting et al., 2014).

Table 1 Standard aCSF

Standard aCSF				
Substances	Concentration stock solution (mM)	MW (g/mol)	Concentration. (mM)	Amount/l
$CaCl_2$ x $2H_2O$	480	147.00	0.5	1.04 ml
$MgSO_4$ x $7H_2O$	260	246.50	7.0	26.9 ml
KH_2PO4	240	136.08	1.2	5.0 ml
KCl	379	74.60	1.9	5.0 ml
NaCl	2540	58.44	95	37.4 ml
$NaHCO_3$		84.01	26	2.18 g
Glucose		198.20	15	2.97 g
Sucrose		342.30	50	17.10 g

Table 2 NMDG-HEPES aCSF

NMDG-HEPES aCSF				
Substances	Concentration stock solution (mM)	MW (g/mol)	Concentration (mM)	Amount/l
$CaCl_2$ x $2H_2O$	2000	147.00	0.5	250 µl

$MgSO_4$ x $7H_2O$	2000	246.50	10	5 ml
KCl		74.60	2.5	0.19 g
$NaHCO_3$		84.01	30	2.52 g
Glucose		198.2	25	4.95 g
NMDG		195.20	93	18.16 g
NaH_2PO_4		138.00	1.2	0.17 g
HEPES		238.30	20	4.77 g
Na-ascorbate		198.00	5	0.99 g
Thiourea		76.10	2	0.15 g
Na-pyruvate		110.00	3	0.33 g

Table 3 Recording aCSF

Recording aCSF				
Substances	Concentration stock solution (mM)	MW (g/mol)	Concentration (mM)	Amount/l
$CaCl_2$ x $2H_2O$	480	147.00	2.4	5 ml
$MgSO_4$ x $7H_2O$	260	246.50	1.3	5 ml
KH_2PO4	240	136.08	1.2	5 ml
KCl	379	74.60	1.89	5 ml
NaCl	2540	58.44	127	50 ml
$NaHCO_3$		84.01	26	2.19 g
Glucose		198.2	15	2.98 g

4.6. Statistical analysis

Statistical calculations were performed with GraphPad Prism 6 (Version 6.01, GraphPad Software). Figures were created with GraphPad Prism 6 and CorelDraw 2019 (Corel Cooperation). Each data set was tested for normality using the Shapiro-Wilk test. If both groups had a normal distribution, differences in number of patchable cells per slice, RMP and AP amplitude between corresponding groups were tested with a t-test. In case normality test failed, a Wilcoxon-Mann-Whitney U test was performed. To test for a difference in the overall number of inputs, each cell was classified as whether an eEPSC was detected after dorsal stimulation or not. The number of cells with input and the overall number of patched cells for each corresponding group were compared with a Chi-Square test. To analyse differences in the mean amplitude and event rate of sEPSC between groups and over time a 2-way analysis of variance (ANOVA) was performed. RMP and AP amplitude were corrected with a factor of two (number of combined comparisons) in a Bonferroni *post-hoc* test. sEPSC amplitude and event rate were corrected with a factor of two in a Bonferroni *post-hoc* test. Levels of statistical significance were categorized as: $p < 0.05$ (*), $p < 0.01$ (**) or $p < 0.001$ (***). The detailed statistical information can be found in every figure legend. P-values are only specified in the text when there is a significant difference between the groups. This was done to increase the readability of the text. Data are expressed as mean +/- standard error of mean (SEM).

5. Results

5.1. Comparison of two distinct age stages of rats

To investigate the viability of spinal cord slices and cell condition of lamina I neurons, I first assessed slice morphology and the electrophysiological properties, respectively. The slices were obtained from animals of two distinct age stages: adolescent (35–40 days old; in total: N = 10 animals, n = 25 slices and 73 cells) and young rats (20–25 days old; in total: N = 9 animals, n = 27 slices and 74 cells). Preparation time varied from 70–120 min, with a mean time of 92 ± 2 min, depending on the number of obtained slices. There was no significant difference in the mean RMP between the age groups ($mean_{Adolescent}$ = –54.1 ± 1.4 mV, $mean_{Young}$ = –54.2 ± 1.2 mV, **Fig. 7** A). A higher AP amplitude was observed in cells from the young age group in comparison to cells from the adolescent age group ($p = 0.0032$, Bonferroni-corrected p-value = 0.0096, $mean_{Adolescent}$ = 59 ± 2mV, $mean_{Young}$ = 67 ± 1.6 mV, **Fig. 7** B). The number of cells

with input from peripheral fibres was similar in both age groups ($input_{Adolescent}$ = 39/73, $input_{Young}$ =48/74, **Fig. 7** C). When assessing the slice viability based on the number of healthy and patchable cells, both groups had an equal number per slice ($mean_{Adolescent}$ = 7.1 ± 0.6, $mean_{Young}$ = 7.2 ± 0.6, **Fig. 7** D).

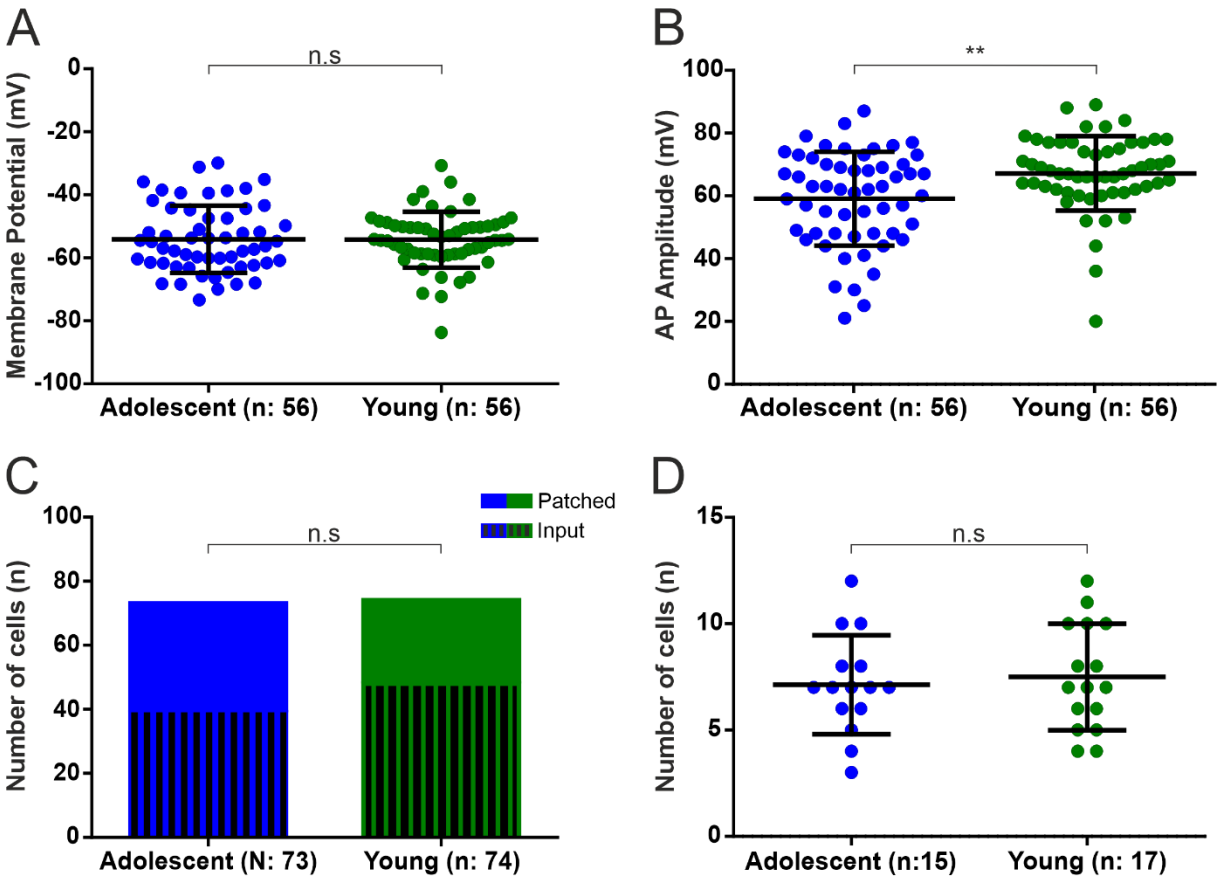

Fig. 7 Assessing spinal cord slice viability and electrophysiological properties of lamina I neurons. Properties were recorded in a whole-cell patch-clamp configuration from lamina I neurons in transversal spinal cord slices of rats from two different age groups. ***A*** RMP of cells recorded in I=0 mode. No significant difference was found between both age groups (p = 0.9479, Bonferroni-corrected p-value ≈ 1). **B** AP amplitude of cells recorded in current-clamp mode, with a significant difference between both age groups (p = 0.0032, Bonferroni-corrected p-value = 0.0064). **C** Number of cells with input from dorsal root stimulation (striped bars) and the total number of patched cells (coloured bar). Cells were recorded in voltage-clamp mode. There was no significant difference between both groups (p = 0.1582). **D** Number of patchable cells per slice fulfilling the morphological criteria for a healthy neuron. No significant difference was found (p = 0.6763).

Cells were recorded in voltage-clamp for 15.5 min to measure action-potential-dependent sEPSC (adolescent: N = 9 animals, n = 11 slices and 17 cells; young: N = 8 animals, n = 13

slices and 18 cells). The amplitude (**Fig. 8** A) and event rate (**Fig. 8** B) of sEPSCs were similar over time and between the two age groups.

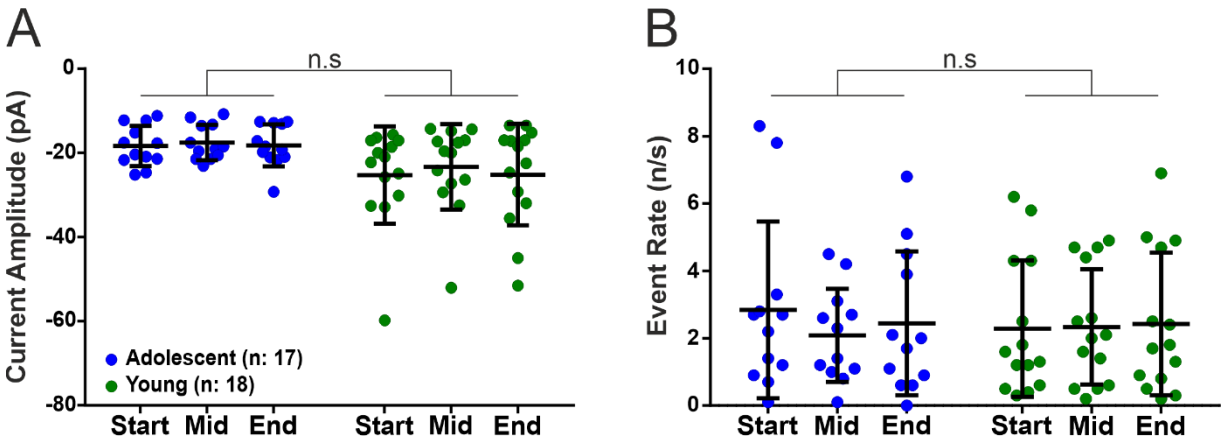

Fig. 8 Comparison of sEPSC of lamina I neurons of young and adolescent rats. sEPSCs were recorded for 15 min in voltage-clamp mode. Amplitude and event rate were analysed for three time intervals at the start (0–3 min), middle (6–9 min) and end (12.5–15.5 min) of each recording. **A** There was no significant difference in the amplitude of the sEPSC, neither over time ($F(2, 48) = 0.7153$, $p = 0.4942$, Bonferroni-corrected p-value = 0.9884) nor between the age groups ($F(1, 24) = 4.285$, p: 0.0494, Bonferroni-corrected p-value = 0.0988). **B** There was no significant difference in the event rate of sEPSCs, neither over time ($F(2, 48) = 1.117$, $p = 0.3357$, Bonferroni-corrected p-value = 0.6714) nor between the age groups ($F(1, 24) = 0.0207$, p: 0.8866, Bonferroni-corrected p-value ≈ 1).

5.2. Probing the NMDG protocol

In an effort to compare the protective abilities of different aCSF solutions, spinal cord slices from adolescent animals were prepared in standard aCSF (in total N = 7 animals, n = 24 slices and 64 cells) or NMDG-HEPES aCSF (in total N = 8 animals, n = 26 slices and 61 cells). Preparation time varied from 60–120 min, with a mean time of 73 ± 4 min, depending on the number of obtained slices. Cells of both groups had a similar RMP ($mean_{Standard}$ = –52.3 ± 1.3 mV, $mean_{NMDG}$ = –54.6 ± 1.4 mV, **Fig. 9** A) and a similar AP amplitude ($mean_{Standard}$ = 67 ± 2 mV, $mean_{NMDG}$ = 67 ± 2 mV, **Fig. 9** B). However, cells of the NMDG group had significantly more input in comparison to the standard group ($p = 0.0034$, $input_{Standard}$ = 39/64, $input_{NMDG}$ =48/61, **Fig. 9** C). When assessing the overall slice viability by counting the number of healthy cells, there was a significant difference between the groups. Slices prepared with NMDG-HEPES aCSF had fewer patchable cells than the slices prepared with standard aCSF (*p = 0.0241,* $mean_{Standard}$ = 7.0 ± 0.8, $mean_{NMDG}$ = 4.6 ± 0.6*,* **Fig. 9** D).

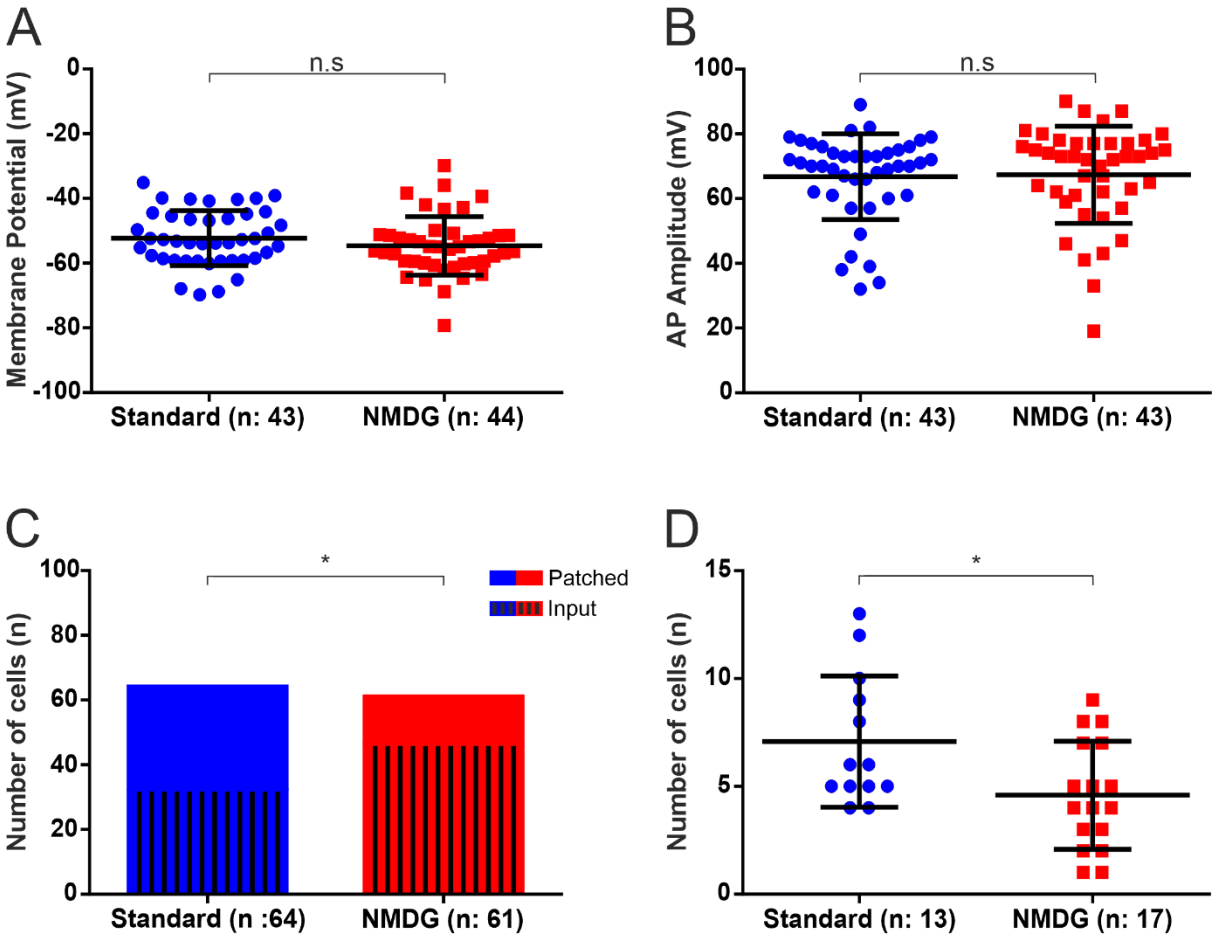

Fig. 9 Assessing spinal cord slice viability and electrophysiological properties of lamina I neurons using different solutions. Properties were recorded in a whole-cell patch-clamp configuration from lamina I neurons in transversal spinal cord slices obtained from male adolescent rats. Slices were prepared either with standard aCSF or NMDG-HEPES aCSF. **A** RMP was recorded in I=0 mode. There was no significant difference between solution groups ($p = 0.2159$, Bonferroni-corrected p-value = 0. 4318). **B** AP amplitude of cells recorded in current-clamp mode. There was no significant difference between the solution groups ($p = 0.5542$, Bonferroni-corrected p-value ≈ 1). **C** Number of cells with input from dorsal root stimulation (striped bars) and the total number of patched cells (coloured bar). There was a significant difference between both groups ($p = 0.0034$). **D** Number of patchable cells per slice fulfilling the morphological criteria for a healthy neuron. A significant difference was found between the groups ($p = 0.0241$).

Cells were recorded in voltage-clamp for 15.5 min to measure action-potential-dependent sEPSC (Standard: N = 6 animals, n = 13 slices and 21 cells; NMDG: N = 7 animals, n = 12 slices and 17 cells). The amplitude (**Fig. 10** A) and event rate (**Fig. 10** B) of sEPSCs were similar over time and between the two groups.

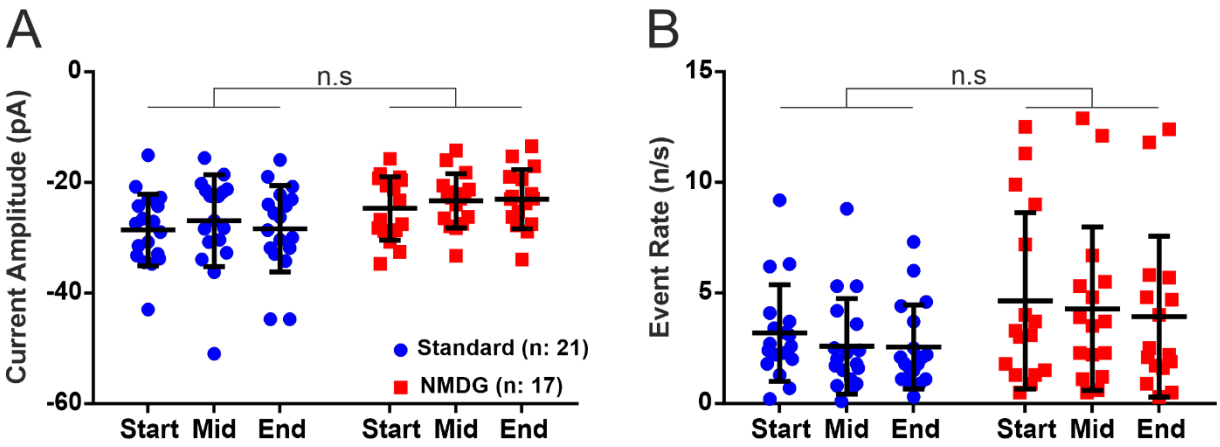

Fig. 10 Comparison of sEPSCs of lamina I neurons exposed to different aCSF solutions. sEPSCs were recorded for 15 min in voltage-clamp mode. Amplitude and event rate were analysed for three time intervals at the start (0–3 min), middle (6–9 min) and end (12.5–15.5 min) of each recording. **A** There was no significant difference in the amplitude of the sEPSC, neither over time ($F(2, 64) = 1.444$, $p = 0.2435$, Bonferroni-corrected p-value = 0.4920) nor between the solution groups ($F(1, 32) = 4.468$, p: 0.0424, Bonferroni-corrected p-value = 0.0848). **B** There was no significant difference in the event rate of sEPSCs, neither over time ($F(2, 64) = 3.877$, $p = 0.0257$, Bonferroni-corrected p-value = 0.0514) nor between the solution groups ($F(1, 32) = 2.326$, p: 0.1370, Bonferroni-corrected p-value = 0.2740).

5.3. Probing an updated NMDG protocol

To evaluate whether a shorter exposure to NMDG-HEPES aCSF is more beneficial for slice protection, spinal cord slices from adolescent animals were prepared with the standard protocol (in total: N = 7 animals, n = 21 slices and 65 cells) or with a short NMDG-r protocol (in total: N = 6 animals, n = 27 slices and 63 cells). Preparation time varied from 65–80 min, with a mean time of 73 ± 1 min, depending on the number of obtained slices.

Cells of both group had a similar RMP ($mean_{Standard}$ = –55.6 ± 1.4 mV, $mean_{NMDG\text{-}r}$ = –55.4 ± 1.1 mV, **Fig. 11** A), AP amplitude ($mean_{Standard}$ = 59 ± 2 mV, $mean_{NNMDG\text{-}r}$ = 58 ± 3 mV, **Fig. 11** B) and number of cells with input ($input_{Standard}$ = 46/65, $input_{NMDG\text{-}r}$ =44/63, **Fig. 11** C). When assessing the overall slice viability by counting the number of healthy cells, the groups showed no significant difference per slice ($mean_{Standard}$ = 7.1 ± 0.9, $mean_{NMDG\text{-}r}$ = 5.9 ± 0.9, **Fig. 11** D).

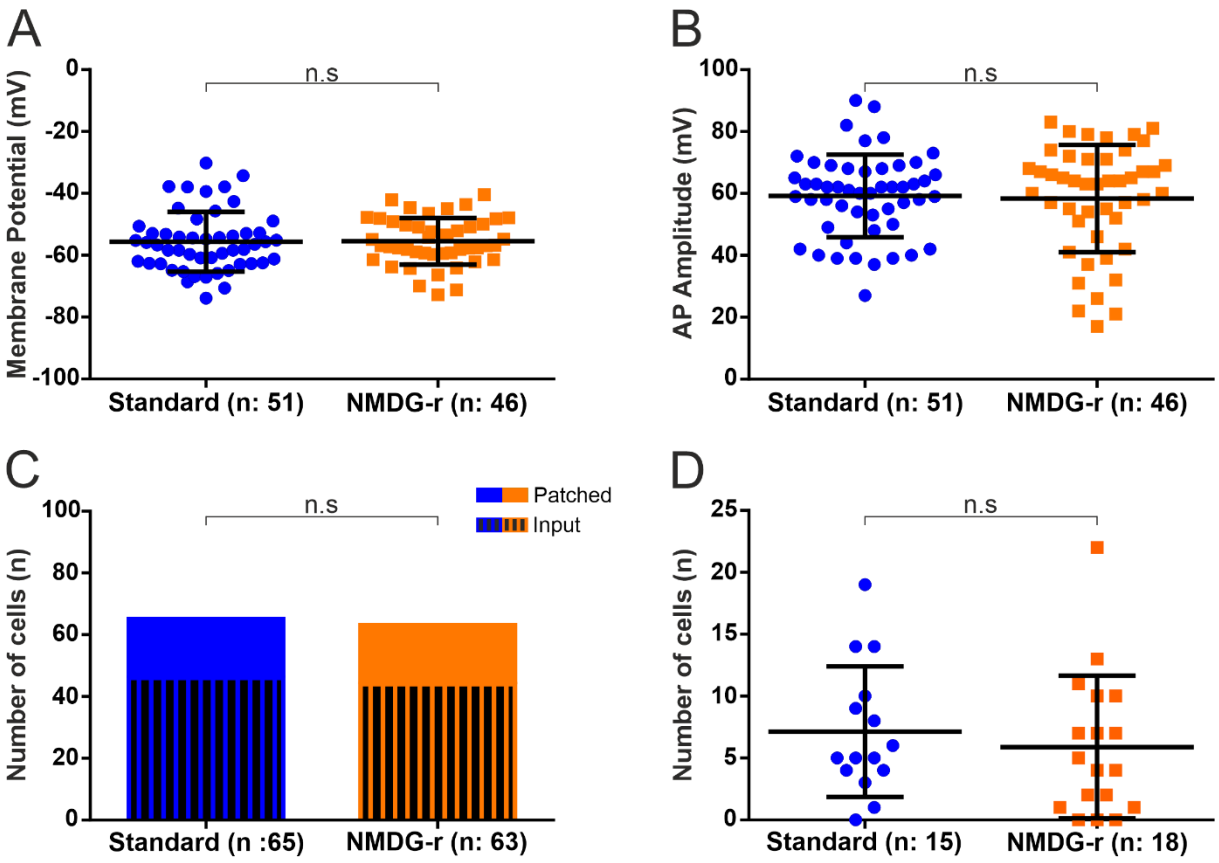

Fig. 11 Assessing spinal cord slice viability and electrophysiological properties of lamina I neurons using different aCSF solutions. Properties were recorded in a whole-cell patch-clamp configuration from lamina I neurons in transversal spinal cord slices obtained from male adolescent rats. Slices underwent a short recovery period either in standard aCSF or in NMDG-aCSF. **A** RMP was recorded in I=0 mode. It was similar between both solution groups ($p = 0.5207$, Bonferroni-corrected p-value ≈ 1). **B** AP amplitude of cells recorded in current-clamp mode. There was no significant difference between both solution groups ($p = 0.6620$, Bonferroni-corrected p-value ≈ 1). **C** Number of cells with input from dorsal root stimulation (striped bars) and the total number of patched cells (coloured bars). Both groups had a similar proportion of input ($p = 0.9085$). **D** Number of patchable cells per slice fulfilling the morphological criteria for a healthy neuron. There was no significant difference between the groups ($p = 0.4141$).

Cells were recorded in voltage-clamp for 15.5 min to measure action-potential-dependent sEPSC (Standard: N = 7 animals, n = 8 slices and 14 cells; NMDG-r: N = 6 animals, n = 12 slices and 17 cells). The amplitude (**Fig. 12** A) and event rate (**Fig. 12** B) of sEPSCs were similar over time and between the two groups.

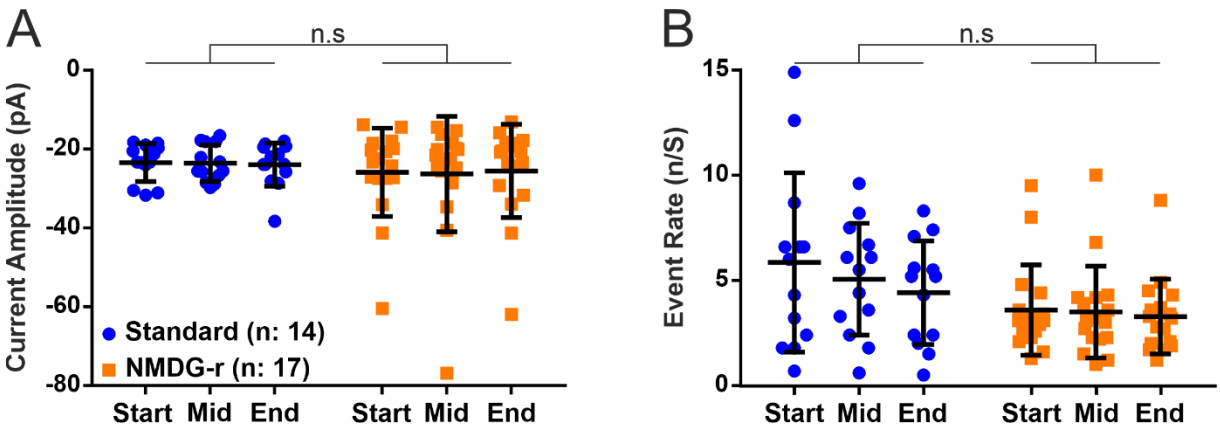

Fig. 12 Comparison of sEPSCs of lamina I neurons using different aCSF solutions. sEPSCs were recorded for 15 min in voltage-clamp mode. Amplitude and event rate were analysed for three time intervals at the start (0–3 min), middle (6–9 min) and end (12.5–15.5 min) of each recording. **A** There was no significant difference in the amplitude of the sEPSC, neither over time (F (2, 56) = 0.80009, p: 0.9231, Bonferroni-corrected p-value: ≈1) nor between the solution groups (F (1, 28) = 0.9390, p: 0.5358, Bonferroni-corrected p-value: ≈1). **B** There was no significant difference in the event rate of sEPSCs, neither over time (F (2, 56) = 3.920, p: 0.0255, Bonferroni-corrected p-value: 0.056) nor between the solution groups solution (F (1, 28) = 3.424, p: 0.0748, Bonferroni-corrected p-value: 0.1496).

6. Discussion

This study aimed to answer two questions: Is there a difference between the viability of spinal cord slices from young and adolescent animals? Does NMDG-HEPES aCSF better preserve spinal cord slice viability than sucrose aCSF?

In the present study, I show that 1. the overall viability and cell condition did not differ between acute spinal cord slices from young and adolescent rats, and 2. the slice viability was significantly reduced in slices from adolescent animals when prepared with NMDG-HEPES aCSF in comparison to sucrose aCSF. The viability could be restored to sucrose aCSF level by reducing the exposure time to NMDG-HEPES aCSF to a short recovery period.

6.1. Slice viability was independent of animal age

The first aim of this study was to investigate whether spinal cord slices obtained from young and adolescent rats are differentially affected by the slice-cutting process itself. During this process ischemic, mechanical and reperfusion injuries are inflicted to the neuronal tissue. There is evidence suggesting a lower viability of brain slices obtained from adult animals as compared to slices obtained from younger animals (Tanaka et al., 2008; Huang and Uusisaari,

2013; Ting et al., 2014). Mitra and Brownstone (2012) also reported similar problems for acute spinal cord slices from adult rodents. Similar observations were made in our own experiments using spinal cord slices from adolescent rats. However, to the best of my knowledge, a quantitative study of spinal cord slice viability of young versus adolescent rats is still missing.

Here, I thus compared acute spinal cord slices from young male rats, age ranging from 20–25 days, with slices from adolescent male rats with an age ranging from 35–40 days. The overall slice viability was assessed by counting healthy, patchable neurons in lamina I of the dorsal horn. To examine the electrophysiological properties of these neurons, the RMP, the AP amplitude, the dynamics of sEPSC and the dorsal root input were determined and compared. Slices were equally viable and electrophysiological properties of neurons were similar in both age groups. Thus, my findings do not support the reports of lower viability in spinal cord slices obtained from adolescent animals. However, a comparison of slice viability between young and adult animals is still missing.

In the present study, the AP amplitude was found to be significantly lower in neurons of slices of the adolescent group. Long-lasting depolarization of the membrane potential can alter activation and conductance of voltage-dependent Na^+ ion channels (Na_V), affecting AP properties and lowering the amplitude (Malenka et al., 1981; Patrick and Waxman, 2007). But since there is no difference of RMP between both groups, this explanation is unlikely. The properties of the action potential highly depend on the activity of voltage-gated Na^+ (Na_V) and K^+ (K_V) channels. A lower number of voltage-gated channels or a different composition of isoforms in adolescent animals could explain the lower amplitude. In young rats (P 3–9), neurons of lamina I/II in the dorsal horn seem to mainly express Na_V 1.2 and 1.3 channels. Around P10 the expression of Na_V 1.2 and 1.3 decreases while the expression of Na_V 1.1 and 1.6 channels increases to a level slightly below or equal to Na_V 1.2 and 1.3. This proportion of Na_V isoforms seems to stay constant after P 20 until P 42 (Blankenship et al., 2013;Hildebrand et al., 2011). Safronov et al. (1999) showed that the amplitude of Na^+ currents triggered by depolarization increased gradually with age (P 0–39). These findings are not in line with my observation that the AP amplitude was lower in adolescent compared to young animals. A difference in isoform proportion of K_V channels could also influence the properties of APs but to date and to the best of my knowledge, an appropriate study is missing. The examination of voltage-dependent channels and AP propagation was beyond the scope of this project but would be an interesting subject for future research.

6.2. NMDG-HEPES aCSF was not superior to sucrose aCSF

Depending on the specific circumstances of the preparation and animal health condition, low slice viability occasionally occurred in all age stages. Slices with the highest viability had 10–12 healthy, patchable cells in lamina I. The average value, however, was 7 cells whereas the slices in the worst condition had less than 5 healthy cells in lamina I. These findings suggested that there is still potential for improvement. Low slice viability in acute slices can alter cytoarchitecture and impair cell function. Any parameters examined during experiments would not reflect physiological conditions. Furthermore, low viability in neuronal tissue can increase the number of animals and the time span needed for an experiment. Therefore, improvements of protective measurements should be implemented whenever possible. In the next step, I thus compared the preservative abilities of a NMDG-HEPES aCSF with a modified sucrose aCSF. Acute spinal cord slices were obtained from adolescent rats for both groups. The NMDG-HEPES aCSF contained NMDG as a NaCl substitute in an attempt to reduce the formation of oedema. HEPES was used as a buffer to keep the pH of the extracellular environment close to physiological level. Additionally, the solution contained ascorbate and thiourea as antioxidants as well as pyruvate to protect the slice against ROS.

There was no significant difference regarding the RMP, dorsal root input and EPSC properties between both groups. However, slices prepared with NMDG-HEPES aCSF were significantly less viable than their counterparts prepared with sucrose aCSF but had significantly more input from the dorsal root. Cells fulfilling the morphological health criteria seemed to have maintained their electrophysiological properties in both aCSFs. The NMDG-HEPES aCSF nevertheless failed to prevent swelling in a large number of cells and was thus ineffective in maintaining or increasing the number of patchable cells. Oedema was observed not only superficially but also deeper within the slice as well as across all laminae of the grey matter. This could indicate a systemic problem rather than just mechanical stress from the slicing procedure.

In studies with neuronal cell cultures, substitution of NaCl with NMDG (Friedman and Haddad, 1994; Chidekel et al., 1997) resulted in a similar morphological preservation as reported for acute slices (Ting et al., 2014; Pan et al., 2015; Avegno et al., 2019). However, it was shown that cells undergo acidification during exposure to NMDG-substituted aCSF. This may be caused by the blockage of the Na^+-proton exchanger, which can no longer utilise the inward flow of one Na^+ ion along the gradient to transport one proton out of the cell (Hartley and Dubinsky, 1993; Sidky and Baimbridge, 1997). Furthermore, an increase of intracellular calcium was observed in cultures exposed to NMDG aCSF (Friedman and Haddad, 1994; Ferreira et al., 1996; Hoener, 2000). The accumulation of calcium ions may contribute to

enzymatic activity inducing protein breakdown, free radical formation and lipid peroxidation (Lipton and Rosenberg, 1994; Brahma et al., 2000). While the substitution of Na^+ with NMDG may preserve morphological features, the apparent acidification and increased intracellular calcium concentration may impair cell function. Ting et al. (2018) propose in their updated NMDG-HEPES aCSF protocol a step wise reintroduction of Na^+ to the acute brain slice to enhance viability. This procedure could also reduce the cell swelling in our spinal cord slices by reducing osmotic stress to the cells. However, this procedure would add another 40 min to the preparation duration.

Zhao et al. (2011) reported that the exposure time of the acute slices to the NMDG aCSF is critical to maintain a balance between preserving morphology and function. A prolonged exposure seemed to produce undesired slice conditions. The researchers reduced the initial recovery period with NMDG-HEPES aCSF from 20–30 min to 10–15 min. However, a detailed description on how morphology or function was altered or improved in comparison to longer recovery durations is missing. The reported time effect of NMDG exposure may also depend on the original condition of the cells or the tissue. In culture, more lesioned spinal cord neurons survived when NaCl was substituted with NMDG, while the prolonged exposure of NMDG was more toxic for unlesioned neurons (Rosenberg et al., 2001). Ting et al. (2018) recommend that the preparation of brain slices in mice should not take longer than 15 min. However, preparation of the spinal cord with intact roots takes up to 75 min, depending on the experience of the experimenter and the size of the animal (age, mouse/rat). It is possible that the prolonged NMDG-exposition during the spinal cord slice preparation, especially with intact roots, exerts toxic effects on the neuronal tissue due to the impairment of overall cell function. However, I found more studies using NMDG-HEPES aCSF for perfusion and/or preparation of acute spinal cord slices (Nashmi et al., 2002; Aresh et al., 2017; Freitag et al., 2019; Hagenston et al., 2019; Petitjean et al., 2019) than studies which used NMDG just for a recovery period (Imlach et al., 2016). Not all of them included an additional recovery period.

As a next step, we examined whether spinal cord slice viability would benefit from a shorter exposure to NMDG-HEPES aCSF. The preparation itself was performed with the standard aCSF followed by a 15 min recovery period in NMDG-HEPES aCSF at 34°C. The slices were finally incubated for another 15 min at 34°C in standard aCSF. This NMDG-r group was compared to a standard group (i.e. only standard sucrose aCSF was used). There were no significant differences in the overall slice viability and any of the electrophysiological properties measured between both groups. The finding that the slice viability of the NMDG-r group was now similar to the standard group seems to support the theory of a time-dependent effect of the NMDG-HEPES aCSF on the overall slice condition. However, the recovery period with

NMDG-HEPES aCSF did not preserve the viability any better than the sucrose aCSF. At this point in time, the data obtained in the present study does not support the replacement of sucrose aCSF with NMDG-HEPES aCSF for the acute spinal cord preparation protocol with intact roots.

Next to NMDG-HEPES aCSF, there are several other possible modifications to the preparation that could be beneficial for slice viability. For example, slicing the brain near freezing point resulted in a firmer tissue allowing a clean cut (Edwards et al., 1989) and reduced oxygen demanding processes (Ivanov and Zilberter, 2011). On the downside, reduction of metabolic processes may also affect pathways linked to cell survival. Recent experiments in which slices were cut close to physiological temperature with a modern slicer resulted in overall healthier morphological and electrophysiological properties in cells of young adult compared to young rodents (Huang and Uusisaari, 2013). Cutting near physiological temperature preserved synaptic structures and function (Bourne et al., 2007; Eguchi et al., 2020). However, the lower rigidity of warm tissue requires a very slow cutting speed with a vertical vibration lower than 0.5 µm. This requirement cannot be fulfilled by all slicers. Hence, physiological temperature slicing should be performed using modern devices only (Huang and Uusisaari, 2013; Ankri et al., 2014). In general, a high-quality slicer might be beneficial for viability by reducing the amount of compression injury due to vertical blade movement. A potential reduction of animals used as well as the shortened project duration always trumps high acquisition costs.

Several researchers also reported improved slice conditions after transcardial perfusion of the animal (Richerson and Messer, 1995;Tanaka et al., 2008; Zhao et al., 2011; Peça and Feng, 2011). Here, blood is replaced in the living but deeply anaesthetised animal with an aCSF in which Na^+ is already substituted. In this way, excitotoxic and ischemic effects can be reduced before mechanical stress is applied to the brain tissue. However, an objective quantification of the advantages of transcardial perfusion prior to the preparation over the standard preparation protocol has not been performed so far.

In the present study, I showed that slices which were exposed to the NMDG-HEPES aCSF during preparation and recovery period had significantly more input in response to dorsal root stimulation compared to the standard aCSF. This could be a result of poor viability in dorsal root ganglions. Injury and inflammation have been shown to increase excitability of dorsal root ganglions (Hu and Xing, 1998; Zhang et al., 1999). Stimulation of the dorsal roots could have triggered action potentials in more afferents resulting in a higher number of recorded input. Furthermore, the prolonged incubation time with NMDG-HEPES aCSF could have led to oedema formation in interneurons of the superficial dorsal horn. Lamina I of the spinal dorsal

horn has two main cell types: Projection neurons sending projections to the ascending tracts to the brain and interneurons which modulate the somatosensory input. In lamina I, this input is mainly from nociceptive Aδ- and C-fibre afferents. Approximately 25% of the interneurons in lamina I are inhibitory GABAergic and partly glycinergic interneurons, whereas about 70% are glutamatergic excitatory interneurons (Todd, 2010, 2017; Polgár et al., 2013). Oedemic interneurons might be more depolarized and thereby more excitable. Hence, stimulation of dorsal root afferents could have triggered activity in more cells, which would have not been activated in healthy conditions. The additional activity of interneurons might have been measured as increased input.

6.3. General

The stability of a patch-clamp recording and its physiological relevance depends on the condition of the cell. Thus, the number of recordings per animal and subsequently the number of required animals per experimental group highly depend on the preservation of the slice viability during the preparation. The effectiveness of a protective aCSF is therefore highly relevant for animal welfare. The applied assay, in which cells with a healthy morphology were counted, was able to give a good overview on the potential number of patchable cells in one slice. Nevertheless, this method was prone to certain inaccuracy. The criteria used to identify a morphologically healthy cell were a diffuse, non-plastic membrane and a non-visible nucleus. In the ideal case, the cell structure was barely detectable from the surrounding tissue. Counting errors might have occurred in which healthy cells would not have been detected at all. In addition, the morphology of the membrane was not an all-or-none criterion and occasionally the classification into healthy or non-healthy was difficult. Cells might have been categorised as healthy although they were already at an early stage of oedema. To reduce these effects, I categorised the cells as conservatively as possible. Furthermore, I was blinded for the solution used and the order of usage was intermingled. Bad slice condition might also be reflected by the number of oedemic cells in a slice. Criteria for oedema was a round and plastic morphology and a clearly visible nucleus. These criteria might be easier to detect and may enable a more reliable categorisation of the cells regarding their condition. Nonetheless, there is still the need for an objective quantification of the viability of acute slices. A potential assay could be the staining of neuronal cell death markers by immunohistochemistry. Apoptosis is a controlled cell death which requires ATP consumption and involves caspase activity. The effector protein for cell death is caspase 3. Typically, the cell undergoes shrinkage during the apoptotic pathway due to breakdown of the cytoskeleton. Finally, the cell is fragmented and removed by

phagocytic cells. In contrast, cell death following oedema formation due to injury is an “accidental” cell death often linked to necrosis. It is induced by ATP depletion and the resulting failure of the Na^+/K^+-pump. As a result, cytosolic calcium increases drastically, inducing the activation of proteases and phospholipases which degrade organelles and the cell membrane. The weakened membrane will eventually rupture, resulting in leakage of the cell interior into the extracellular space (Fricker et al., 2018). Necroptosis is a hybrid between the apoptotic and the necrotic death pathways and is often linked to inflammation. Activation of death receptors results into the activation of serine/threonine-protein kinase (RIP) 1 and 3. Both forming a complex called necrosome, which initiates rupturing of organelle- and plasma membranes, resulting in release of damage-associated molecular patterns responsible for recruiting immune cells to the inflamed tissue (Khan et al., 2014; Orozco and Oberst, 2017). While apoptotic and necroptotic cell death occurs after spinal cord injury, their makers might not be suitable for acute slices. Acute spinal cord slices are mostly used within 6–8 hours after slicing. Popular markers for apoptosis or necroptosis such as caspase 3 and 8 (Takagi et al., 2003; Kakinohana et al., 2011) or RIP3 (Kanno et al., 2015; Fan et al., 2016) are only detectable 8 hours after spinal cord injury. In a pilot experiment testing popular necroptosis marker such as cleaved caspase 3 and RIP3, we performed a hypoxic challenge in spinal cord slices. We were not able to detect a measurable difference in fluorescence intensity after 2 or 4 hours without oxygen in comparison to control slices with standard oxygenation.

Etidium Bromide (EB) or Propidium iodide (PI) are often used as markers for apoptotic or necrotic cells. They are fluorescent dyes working as intercalating agents binding to DNA and RNA. In theory, the dyes are unable to diffuse through the membranes of healthy cells and only pass through leaky membranes of apoptotic or necrotic cells (Monette et al., 1998; Mironova et al., 2007; Sayas et al., 2015). When we monitored EB staining of acute spinal cord slices in real-time, EB not only stained oedemic cells but also cells with a healthy looking morphology. These cells were – judging by their morphology – non-neuronal cells. This is in line with literature, as it seems that EB can also pass through hemi-channels of healthy astrocytes (Yin et al., 2018; Slavi et al., 2018). Therefore, EB should not be used as a specific marker for dying cells. However, EB or PI staining could be combined with staining for the neuronal nuclear protein (NeuN). NeuN is a protein associated with cell nuclei and the perinuclear cytoplasm. Its antibodies can identify the majority of neuronal tissue while it does not bind to any other forms of tissue (Gusel'nikova and Korzhevskiy, 2015). Both markers combined could probably be used to identify apoptotic or necrotic neurons and count their number for a specific region of interest.

7. Summary

In summary, I found no difference in the viability of acute spinal cord slices between young (P 20–25) and adolescent (P 35 – 40) male rats. These findings do not support claims of bad condition in slices from adolescent animals. A specific treatment for slices from this age stage is thereby not necessary. Preparation and recovery of spinal cord slices in NMDG-HEPES aCSF reduced viability but increased dorsal root input in form of eEPSCs in lamina I neurons. When exposure time to NMDG-HEPES aCSF was reduced to a short recovery incubation, viability and electrophysiological properties were similar to the control group. Based on the results of this study, I do not recommend the usage of NMDG-HEPES aCSF for acute spinal cord slice preparation.

8. Appendix

8.1. Zusammenfassung

Akute Hirnschnitte sind ein wichtiges Modell in der Forschung an neuronalen Netzwerken. Das Modell ist gut geeignet für die Anwendung von bewegungsanfälligen elektrophysiologischen Techniken sowie pharmakologische Untersuchungen. Das Gewebe kann jedoch während der Präparation ischämische Verletzungen erleiden. Vor allem Schnitte von älteren Tieren seien laut Berichten anfälliger für die Verletzungen und ihre Überlebensfähigkeit sei gering. Einer der effektivsten Methoden, um die Überlebensfähigkeit der Schnitte zu bewahren, ist die Modifizierung der artifiziellen Gehirn-Rückenmark-Flüssigkeit (aCSF). Eine NMDG-HEPES aCSF angereichert mit Antioxidantien wurde konzipiert um Ödembildung, Versäuerung und oxidativen Stress im Gewebe zu reduzieren. Die NMDG-HEPEs aCSF findet zwar bereits Verwendung in der Herstellung von gesunden Hirnschnitten, positive Effekte für die Überlebensfähigkeit von Rückenmarksschnitten sind jedoch noch nicht untersucht. Das Ziel meiner Studie war es, die Effektivität von NMDG-HEPES aCSF zur Erhaltung der Überlebensfähigkeit von akuten Rückenmarksschnitten von adoleszenten männlichen Ratten zu testen.

Ein Vergleich der Überlebensfähigkeit der Schnitte von jungen (20–25 Tage) und adoleszenten (35–40 Tage) Tieren zeigte jedoch keinen Unterschied auf. Auch die elektrophysiologischen Eigenschaften von Neuronen in Lamina I beider Gruppen waren gleich. Die Verwendung von NMDG-HEPES aCSF für die Schnitt-Präparation zeigte keinerlei Vorteile im Vergleich zur

modifizierten Zucker aCSF. Im Gegenteil, die Schnitte zeigten eine signifikant geringere Überlebensfähigkeit, die aber durch die Verkürzung der Expositionszeit in NMDG-HEPES aCSF wiederhergestellt werden konnte. Zusammengefasst war NMDG-HEPES aCSF nicht effektiver als traditionelle Zucker aCSF darin, die Überlebensfähigkeit der Rückenmarkschnitte zu bewahren.

8.2. List of figures

8.3. List of tables

8.4. List of boxes

8.5. Abbrevations

Δ	difference in values between point in times
aCSF	artifical cerebrospinal fluid
ANOVA	analysis of variance
AP	action potential
C_M	capactior element of the membrane

HEPES	4-(2-hydroxyethyl)-1-piperazineethanesulfonic acid
I_{max}	initial transient current
K^+	potassium
K_V	voltage gated potassium channel
N	sample size (animal)
n	sample size (slice or cell)
Na^+	Na^+
Na_V	voltage gated Na^+ channel
NMDG	N-methyl-D-glucamine
p	probability that differences between groups is by chance
P	postnatal days
RC	resistor-capacitor element
R_M	resistor element of the membrane
RMP	resting membrane potential
ROS	radical oxygen species
R_S	serial resistance
sEPSC	spontaneous excitatory postsynaptic currents
U	potential

8.6. List of references

Aghajanian GK, Rasmussen K (1989) Intracellular studies in the facial nucleus illustrating a simple new method for obtaining viable motoneurons in adult rat brain slices. Synapse 3:331-338.

Andersen P (1981) Brain slices — a neurobiological tool of increasing usefulness. Cell 4:53-56.

Ankri L, Yarom Y, Uusisaari MY (2014) Slice it hot: acute adult brain slicing in physiological temperature. J Vis Expe52068.

Anzini M, Chelini A, Mancini A, Cappelli A, Frosini M, Ricci L, Valoti M, Magistretti J, Castelli L, Giordani A, Makovec F, Vomero S (2010) Synthesis and biological evaluation of amidine, guanidine, and thiourea derivatives of 2-amino(6-trifluoromethoxy)benzothiazole as neuroprotective agents potentially useful in brain diseases. J Med Chem 53:734-744.

Aresh B, Freitag FB, Perry S, Blümel E, Lau J, Franck MCM, Lagerström MC (2017) Spinal cord interneurons expressing the gastrin-releasing peptide receptor convey itch through VGLUT2-mediated signaling. Pain 158:945-961.

Avegno EM, Middleton JW, Gilpin NW (2019) Synaptic GABAergic transmission in the central amygdala (CeA) of rats depends on slice preparation and recording conditions. Physiol Rep 7:e14245.

Berger AJ (1990) Recent advances in respiratory neurobiology using in vitro methods. Am J Physiol 259:L24-L29.

Bican O, Minagar A, Pruitt AA (2013) The spinal cord: a review of functional neuroanatomy. Neurol Clin 31:1-18.

Blankenship ML, Coyle DE, Baccei ML (2013) Transcriptional expression of voltage-gated Na^+ and voltage-independent K+ channels in the developing rat superficial dorsal horn. Neuroscience 231:305-314.

Blumenfeld KS, Welsh FA, Harris VA, Pesenson MA (1992) Regional expression of c-fos and heat shock protein-70 mRNA following hypoxia-ischemia in immature rat brain. J Cereb Blood Flow Metab 12:987-995.

Bourne JN, Kirov SA, Sorra KE, Harris KM (2007) Warmer preparation of hippocampal slices prevents synapse proliferation that might obscure LTP-related structural plasticity. Neuropharmacology 52:55-59.

Brahma B, Forman RE, Stewart EE, Nicholson C, Rice ME (2000) Ascorbate inhibits edema in brain slices. J Neurochem 74:1263-1270.

Brockhaus J, Dressel D, Herold S, Deitmer JW (2004) Purinergic modulation of synaptic input to Purkinje neurons in rat cerebellar brain slices. Eur J Neurosci 19:2221-2230.

Brune T, Deitmer JW (1995) Intracellular acidification and Ca2+ transients in cultured rat cerebellar astrocytes evoked by glutamate agonists and noradrenaline. Glia 14:153-161.

Cahalan M, Neher E (1992) Patch clamp techniques: an overview. Methods Enzymol 207:3-14.

Chidekel AS, Friedman JE, Haddad GG (1997) Anoxia-induced neuronal injury: role of Na+ entry and Na+-dependent transport. Exp Neurol 146:403-413.

Cox BA, Johnson SW (1998) Nitric oxide facilitates N-methyl-D-aspartate-induced burst firing in dopamine neurons from rat midbrain slices. Neurosci Lett 255:131-134.

Dingledine R, Dodd J, Kelly JS (1980) The in vitro brain slice as a useful neurophysiological preparation for intracellular recording. J Neurosci Methods 2:323-362.

Drdla R, Gassner M, Gingl E, Sandkühler J (2009) Induction of synaptic long-term potentiation after opioid withdrawal. Science 325:207-210.

Dykens JA, Stern A, Trenkner E (1987) Mechanism of kainate toxicity to cerebellar neurons in vitro is analogous to reperfusion tissue injury. J Neurochem 49:1222-1228.

Edwards FA, Konnerth A, Sakmann B, Takahashi T (1989) A thin slice preparation for patch clamp recordings from neurones of the mammalian central nervous system. Pflugers Arch 414:600-612.

Egert U, Heck D, Aertsen A (2002) Two-dimensional monitoring of spiking networks in acute brain slices. Exp Brain Res 142:268-274.

Eguchi K, Velicky P, Hollergschwandtner E, Itakura M, Fukazawa Y, Danzl JG, Shigemoto R (2020) Advantages of acute brain slices prepared at physiological temperature in the characterization of synaptic functions. Front Cell Neurosci 14:63.

Fan H, Zhang K, Shan L, Kuang F, Chen K, Zhu K, Ma H, Ju G, Wang YZ (2016) Reactive astrocytes undergo M1 microglia/macrohpages-induced necroptosis in spinal cord injury. Mol Neurodegener 11:14.

Feig S, Lipton P (1990) N-methyl-D-aspartate receptor activation and Ca2+ account for poor pyramidal cell structure in hippocampal slices. J Neurochem 55:473-483.

Ferreira IL, Duarte CB, Carvalho AP (1996) Ca^{2+} influx through glutamate receptor-associated channels in retina cells correlates with neuronal cell death. Eur J Pharmacol 302:153-162.

Freitag FB, Ahemaiti A, Jakobsson JET, Weman HM, Lagerström MC (2019) Spinal gastrin releasing peptide receptor expressing interneurons are controlled by local phasic and tonic inhibition. Sci Rep 9:16573.

Fricker M, Tolkovsky AM, Borutaite V, Coleman M, Brown GC (2018) Neuronal cell death. Physiol Rev 98:813-880.

Friedman JE, Haddad GG (1994) Removal of extracellular Na^{+} prevents anoxia-induced injury in freshly dissociated rat CA1 hippocampal neurons. Brain Res 641:57-64.

Gilmer LK, Ansari MA, Roberts KN, Scheff SW (2010) Age-related changes in mitochondrial respiration and oxidative damage in the cerebral cortex of the Fischer 344 rat. Mech Ageing Dev 131:133-143.

Grafe MR (1994) Developmental changes in the sensitivity of the neonatal rat brain to hypoxic/ischemic injury. Brain Res 653:161-166.

Gruber-Schoffnegger D, Drdla-Schutting R, Honigsperger C, Wunderbaldinger G, Gassner M, Sandkühler J (2013) Induction of thermal hyperalgesia and synaptic long-term potentiation in the spinal cord lamina I by TNF-α and IL-1β is mediated by glial cells. J Neurosci 33:6540-6551.

Gusel'nikova VV, Korzhevskiy DE (2015) NeuN as a neuronal nuclear antigen and neuron differentiation marker. Acta Naturae 7:42-47.

Hagenston AM, Ayed SB, Bading H (2019) Afferent fiber activity-induced cytoplasmic calcium signaling in parvalbumin-positive inhibitory interneurons of the spinal cord dorsal horn. Math Biosci.

Hartley Z, Dubinsky JM (1993) Changes in intracellular pH associated with glutamate excitotoxicity. J Neurosci 13:4690-4699.

Hildebrand ME, Mezeyova J, Smith PL, Salter MW, Tringham E, Snutch TP (2011) Identification of Na^+ channel isoforms that mediate action potential firing in lamina I/II spinal cord neurons. Mol Pain 7:67.

Hoener MC (2000) Role played by Na^+ in activity-dependent secretion of neurotrophins - revisited. Eur J Neurosci 12:3096-3106.

Hu SJ, Xing J-L (1998) An experimental model for chronic compression of dorsal root ganglion produced by intervertebral foramen stenosis in the rat. Pain 77:15-23.

Huang S, Uusisaari MY (2013) Physiological temperature during brain slicing enhances the quality of acute slice preparations. Front Cell Neurosci 7:48.

Ikonomidou C, Mosinger JL, Salles KS, Labruyere J, Olney JW (1989) Sensitivity of the developing rat brain to hypobaric/ischemic damage parallels sensitivity to N-methyl-aspartate neurotoxicity. J Neurosci 9:2809-2818.

Imlach WL, Bhola RF, Mohammadi SA, Christie MJ (2016) Glycinergic dysfunction in a subpopulation of dorsal horn interneurons in a rat model of neuropathic pain. Sci Rep 6:37104.

Itoh T, Imano M, Nishida S, Tsubaki M, Mizuguchi N, Hashimoto S, Ito A, Satou T (2013) Increased apoptotic neuronal cell death and cognitive impairment at early phase after traumatic brain injury in aged rats. Brain Struct Funct 218:209-220.

Ivanov A, Zilberter Y (2011) Critical state of energy metabolism in brain slices: the principal role of oxygen delivery and energy substrates in shaping neuronal activity. Front Neuroenergetics 3:9.

Jaffe EH, Marty A, Schulte A, Chow RH (1998) Extrasynaptic vesicular transmitter release from the somata of substantia nigra neurons in rat midbrain slices. J Neurosci 18:3548-3553.

Kakinohana M, Kida K, Minamishima S, Atochin DN, Huang PL, Kaneki M, Ichinose F (2011) Delayed paraplegia after spinal cord ischemic injury requires caspase-3 activation in mice. Stroke 42:2302-2307.

Kaneda M, Nakamura H, Akaike N (1988) Mechanical and enzymatic isolation of mammalian CNS neurons. Neurosci Res 5:299-315.

Kanno H, Ozawa H, Tateda S, Yahata K, Itoi E (2015) Upregulation of the receptor-interacting protein 3 expression and involvement in neural tissue damage after spinal cord injury in mice. BMC Neurosci 16:62.

Khan N, Lawlor KE, Murphy JM, Vince JE (2014) More to life than death: molecular determinants of necroptotic and non-necroptotic RIP3 kinase signaling. Curr Opin Immunol 26:76-89.

Knowles WD, Schwartzkroin PA (1981) Local circuit synaptic interactions in hippocampal brain slices. J Neurosci 1:318-322.

Konopacki J, MacIver MB, Bland BH, Roth SH (1987) Carbachol-induced EEG 'theta' activity in hippocampal brain slices. Brain Res 405:196-198.

Kronschläger M, Drdla-Schutting R, Gassner M, Honsek S, Teuchmann HL, Sandkühler J (2016) Gliogenic LTP spreads widely in nociceptive pathways. Science 354:1144-1148.

Liang D, Bhatta S, Gerzanich V, Simard JM (2007) Cytotoxic edema: mechanisms of pathological cell swelling. Neurosurg Focus 22:E2.

Lipton SA, Rosenberg PA (1994) Excitatory amino acids as a final common pathway for neurologic disorders. N Engl J Med 330:613-622.

Liu D, Thangnipon W, McAdoo DJ (1991) Excitatory amino acids rise to toxic levels upon impact injury to the rat spinal cord. Brain Res 547:344-348.

Liu D, Xu G-Y, Pan E, McAdoo DJ (1999) Neurotoxicity of glutamate at the concentration released upon spinal cord injury. Neuroscience 93:1383-1389.

Liu MG, Chen XF, He T, Li Z, Chen J (2012) Use of multi-electrode array recordings in studies of network synaptic plasticity in both time and space. Neurosci Bull 28:409-422.

MacGregor DG, Chesler M, Rice ME (2001) HEPES prevents edema in rat brain slices. Neurosci Lett 303:141-144.

Mainen ZF, Maletic-Savatic M, Shi S-H, Hayashi Y, Malinow R, Svoboda K (1999) Two-photon imaging in living brain slices. Methods 18:231-239.

Malenka RC, Kocsis JD, Ransom BR, Waxman SG (1981) Modulation of parallel fiber excitability by postsynaptically mediated changes in extracellular potassium. Science 214:339-341.

Marvizón JC, Martínez V, Grady EF, Bunnett NW, Mayer EA (1997) Neurokinin 1 receptor internalization in spinal cord slices induced by dorsal root stimulation is mediated by NMDA receptors. J Neurosci 17:8129-8136.

McDonald JW, Silverstein FS, Johnston MV (1988) Neurotoxicity of N-methyl-D-aspartate is markedly enhanced in developing rat central nervous system. Brain Res 459:200-203.

Mironova EV, Evstratova AA, Antonov SM (2007) A fluorescence vital assay for the recognition and quantification of excitotoxic cell death by necrosis and apoptosis using confocal microscopy on neurons in culture. J Neurosci Methods 163:1-8.

Mitra P, Brownstone RM (2012) An in vitro spinal cord slice preparation for recording from lumbar motoneurons of the adult mouse. J Neurophysiol 107:728-741.

Molleman A (2003) Patch clamping - An introductory guide to patch clamp electrophysiology. John Wiley & Sons, Ltd.

Monette R, Small DL, Mealing G, Morley P (1998) A fluorescence confocal assay to assess neuronal viability in brain slices. Brain Res Brain Res Protoc 2:99-108.

Nashmi R, Velumian AA, Chung I, Zhang L, Agrawal SK, Fehlings MG (2002) Patch-clamp recordings from white matter glia in thin longitudinal slices of adult rat spinal cord. J Neurosci Methods 117:159-166.

Navarro A, SÃ¡nchez Del Pino MJ, GÃ³mez C, Peralta JL, Boveris A (2002) Behavioral dysfunction, brain oxidative stress, and impaired mitochondrial electron transfer in aging mice. Am J Physiol Regul Integr Comp Physiol 282:R985-R992.

Nicholls D, Attwell D (1990) The release and uptake of excitatory amino acids. Trends Pharmacol Sci 11:462-468.

Orozco S, Oberst A (2017) RIPK3 in cell death and inflammation: the good, the bad, and the ugly. Immunol Rev 277:102-112.

Pan G, Li Y, Geng HY, Yang J-M, Li KX, Li X-M (2015) Preserving GABAergic interneurons in acute brain slices of mice using the N-methyl-*D*-glucamine-based artificial cerebrospinal fluid method. Neurosci Bull 31:265-270.

Patrick HT, Waxman SG (2007) Inactivation properties of Na^+ channel $Na_v1.8$ maintain action potential amplitude in small DRG neurons in the context of depolarization. Mol Pain 3:12.

Peça J, Feng G (2011) Neuroscience: When lights take the circuits out. Nature 477:165-166.

Petitjean H, Bourojeni B, Tsao D, Davidova A, Sotocinal SG, Mogil JS, Kania A, Sharif-Naeini R (2019) Recruitment of spinoparabrachial neurons by dorsal horn calretinin neurons. Cell Rep 28:1429-1438.

Polgár E, Durrieux C, Hughes DI, Todd AJ (2013) A quantitative study of inhibitory interneurons in laminae I-III of the mouse spinal dorsal horn. PLoS One 8:e78309.

Prehn JH (1998) Mitochondrial transmembrane potential and free radical production in excitotoxic neurodegeneration. Naunyn Schmiedebergs Arch Pharmacol 357:316-322.

Rao SD, Yin HZ, Weiss JH (2003) Disruption of glial glutamate transport by reactive oxygen species produced in motor neurons. J Neurosci 23:2627-2633.

Reischer G, Heinke B, Sandkühler J (2020) Interferon-γ facilitates the synaptic transmission between primary afferent C-fibres and lamina I neurons in the rat spinal dorsal horn via microglia activation. Mol Pain 16:1-12.
Rexed B (1954) A cytoarchitectonic atlas of the spinal cord in the cat. J Comp Neurol 100:297-379.

Rice ME (1999) Use of ascorbate in the preparation and maintenance of brain slices. Methods 18:144-149.

Richerson GB, Messer C (1995) Effect of composition of experimental solutions on neuronal survival during rat brain slicing. Exp Neurol 131:133-143.

Roberts EL, Jr., Chih CP (1997) The influence of age of pH regulation in hippocampal slices before, during, and after anoxia. J Cereb Blood Flow Metab 17:560-566.

Rosenberg LJ, Emery DG, Lucas JH (2001) Effects of Na^+ and chloride on neuronal survival after neurite transection. J Neuropathol Exp Neurol 60:33-48.

Rungta RL, Choi HB, Tyson JR, Malik A, Dissing-Olesen L, Lin PJC, Cain SM, Cullis PR, Snutch TP, MacVicar BA (2015) The cellular mechanisms of neuronal swelling underlying cytotoxic edema. Cell 161:610-621.

Safronov BV, Wolff M, Vogel W (1999) Axonal expression of Na^+ channels in rat spinal neurones during postnatal development. J Physiol 514:729-734.

Sakmann B, Neher E (1984) Patch clamp techniques for studying ionic channels in excitable membranes. Annu Rev Physiol 46:455-472.

Sarvey JM, Burgard EC, Decker G (1989) Long-term potentiation: studies in the hippocampal slice. J Neurosci Methods 28:109-124.

Sasaki T, Awaji T, Shimada K, Sasaki H (2018) Increased levels of reactive oxygen species in brain slices after transient hypoxia induced by a reduced oxygen supply. Neuropsychiatry.

Sayas E, García-López F, Serrano R (2015) Toxicity, mutagenicity and transport in saccharomyces cerevisiae of three popular DNA intercalating fluorescent dyes. Yeast 32:595-606.

Schwartzkroin PA, Mathers LH (1978) Physiological and morphological identification of a nonpyramidal hippocampal cell type. Brain Res 157:1-10.

Sidky AO, Baimbridge KG (1997) Calcium homeostatic mechanisms operating in cultured postnatal rat hippocampal neurones following flash photolysis of nitrophenyl-EGTA. J Physiol 504 (Pt 3):579-590.

Siklós L, Kuhnt U, Párducz A, Szerdahelyi P (1997) Intracellular calcium redistribution accompanies changes in total tissue Na+, K+ and water during the first two hours of in vitro incubation of hippocampal slices. Neuroscience 79:1013-1022.

Slavi N, Toychiev AH, Kosmidis S, Ackert J, Bloomfield SA, Wulff H, Viswanathan S, Lampe PD, Srinivas M (2018) Suppression of connexin 43 phosphorylation promotes astrocyte survival and vascular regeneration in proliferative retinopathy. Proc Natl Acad Sci U S A 115:E5934-E5943.

Staley KJ, Otis TS, Mody I (1992) Membrane properties of dentate gyrus granule cells: comparison of sharp microelectrode and whole-cell recordings. J Neurophysiol 67:1346-1358.

Stett A, Egert U, Guenther E, Hofmann F, Meyer T, Nisch W, Haemmerle H (2003) Biological application of microelectrode arrays in drug discovery and basic research. Anal Bioanal Chem 377:486-495.

Swanson RA, Farrell K, Simon RP (1995) Acidosis causes failure of astrocyte glutamate uptake during hypoxia. J Cereb Blood Flow Metab 15:417-424.

Takagi T, Takayasu M, Mizuno M, Yoshimoto M, Yoshida J (2003) Caspase activation in neuronal and glial apoptosis following spinal cord injury in mice. Neurol Med Chir (Tokyo) 43:20-29.

Tanaka Y, Tanaka Y, Furuta T, Yanagawa Y, Kaneko T (2008) The effects of cutting solutions on the viability of GABAergic interneurons in cerebral cortical slices of adult mice. J Neurosci Methods 171:118-125.

Tian L, Cai Q, Wei H (1998) Alterations of antioxidant enzymes and oxidative damage to macromolecules in different organs of rats during aging. Free Radic Biol Med 24:1477-1484.

Ting JT, Daigle TL, Chen Q, Feng G (2014) Acute brain slice methods for adult and aging animals: application of targeted patch clamp analysis and optogenetics. Methods Mol Biol 1183:221-242.

Ting JT, Lee BR, Chong P, Soler-Llavina G, Cobbs C, Koch C, Zeng H, Lein E (2018) Preparation of acute brain slices using an optimized *N*-Methyl-D-glucamine protective recovery method. J Vis Exp.

Todd AJ (2010) Neuronal circuitry for pain processing in the dorsal horn. Nat Rev Neurosci 11:823-836.

Todd AJ (2017) Identifying functional populations among the interneurons in laminae I-III of the spinal dorsal horn. Mol Pain 13:1744806917693003.

Towfighi J, Mauger D, Vannucci RC, Vannucci SJ (1997) Influence of age on the cerebral lesions in an immature rat model of cerebral hypoxia-ischemia: a light microscopic study. Brain Res Dev Brain Res 100:149-160.

Trotti D, Danbolt NC, Volterra A (1998) Glutamate transporters are oxidant-vulnerable: a molecular link between oxidative and excitotoxic neurodegeneration? Trends Pharmacol Sci 19:328-334.

Tsai KL, Wang SM, Chen CC, Fong TH, Wu ML (1997) Mechanism of oxidative stress-induced intracellular acidosis in rat cerebellar astrocytes and C6 glioma cells. J Physiol 502 (Pt 1):161-174.

Volterra A, Trotti D, Floridi S, Racagni G (1994) Reactive oxygen species inhibit high-affinity glutamate uptake: molecular mechanism and neuropathological implications. Ann N Y Acad Sci 738:153-162.

Yager JY, Shuaib A, Thornhill J (1996) The effect of age on susceptibility to brain damage in a model of global hemispheric hypoxia-ischemia. Brain Res Dev Brain Res 93:143-154.

Ye JH, Zhang J, Xiao C, Kong JQ (2006) Patch-clamp studies in the CNS illustrate a simple new method for obtaining viable neurons in rat brain slices: glycerol replacement of NaCl protects CNS neurons. J Neurosci Methods 158:251-259.

Yin X, Feng L, Ma D, Yin P, Wang X, Hou S, Hao Y, Zhang J, Xin M, Feng J (2018) Roles of astrocytic connexin-43, hemichannels, and gap junctions in oxygen-glucose deprivation/reperfusion injury induced neuroinflammation and the possible regulatory mechanisms of salvianolic acid B and carbenoxolone. J Neuroinflammation 15:97.

Zhang J-M, Song X-J, LaMotte RH (1999) Enhanced excitability of sensory neurons in rats with cutaneous hyperalgesia produced by chronic compression of the dorsal root ganglion. J Neurophysiol 82:3359-3366.

Zhao S, Ting JT, Atallah HE, Qiu L, Tan J, Gloss B, Augustine GJ, Deisseroth K, Luo M, Graybiel AM, Feng G (2011) Cell-typ specific channelrhodopsin-2 transgenic mice for optogenetic dissection of neural circuitry function. Nat Methods 8:745-752.

Zhu C, Wang X, Xu F, Bahr BA, Shibata M, Uchiyama Y, Hagberg H, Blomgren K (2005) The influence of age on apoptotic and other mechanisms of cell death after cerebral hypoxia-ischemia. Cell Death Differ 12:162-176.